Tectonics®

RESEARCH ARTICLE
10.1029/2024TC008689

Shale Tectonics in the Hyperextended Continental Margin of the Niger Delta

V. Spina[1], J. I. Soto[2,3], J.-C. Ringenbach[4], and S. Mazzoli[5]

[1]Deepwater Reservoir Management Department, TotalEnergies Nigeria, Lagos, Nigeria, [2]Departamento de Geodinámica, University of Granada, Granada, Spain, [3]Bureau of Economic Geology, Jackson School of Geosciences, The University of Texas at Austin, University Station, Austin, TX, USA, [4]TotalEnergies SE, Pau, France, [5]Geology Division, School of Science and Technology, University of Camerino, Camerino, Italy

Abstract Based on the interpretation of a large seismic data set, we provide a comprehensive description of the structures affecting the entire Niger Delta, from the onshore domain to the deep-offshore. The shale-dominated delta lies on a divergent segment of the west African passive margin. The delta is underlain by Lower Cretaceous oceanic crust offshore, transitioning landwards to the distal margin and the necking domains of a hyperextended continental lithosphere. The southward progradation of the delta over poorly consolidated Paleocene to Eocene shales facilitated their mobilization since the Early Miocene. Thick shales accumulated over a structural depression, where limited portions of exhumed mantle have been interpreted. The shales are characterized by overpressure conditions, which can be related to both rapid burial and hydrocarbon expulsion. The top of overpressure migrated over time and progressively truncates older successions toward the continent. The downslope flow of shales led to the formation of shale rollers, ridges, and other mobile-shale structures such as complex anticlines and walls. These structures are associated with minibasins filled by Miocene to the Quaternary growth strata. Within the transitional zone and the outer fold–thrust belt, the shales reduced their mobility. Updip extension, which started in Paleogene times, was transferred toward the toe of the gravitational system since the Late Miocene. The magnitude of updip extension is about the double of shortening in the outer fold–thrust belt. Strain unbalance at the scale of the gravitational system results from gravitational spreading being partially accommodated by tectonic (i.e., lateral) compaction of the shales.

Key Points:

- The Niger Delta is controlled by the interaction of gravity-driven processes and the architecture of a hyperextended continental margin
- Structures formed by mobile shales with minibasins and diapirs resemble those formed in salt systems
- The gravity-linked system of mobile shales has greater and older updip extension compared to shortening in the deepwater fold–thrust belt

Supporting Information:

Supporting Information may be found in the online version of this article.

Correspondence to:

S. Mazzoli,
stefano.mazzoli@unicam.it

Citation:

Spina, V., Soto, J. I., Ringenbach, J.-C., & Mazzoli, S. (2025). Shale tectonics in the hyperextended continental margin of the Niger Delta. *Tectonics*, *44*, e2024TC008689. https://doi.org/10.1029/2024TC008689

Received 30 OCT 2024
Accepted 26 JUN 2025

Author Contributions:

Conceptualization: V. Spina, J. I. Soto, S. Mazzoli
Data curation: V. Spina
Formal analysis: V. Spina, J. I. Soto, J.-C. Ringenbach
Funding acquisition: V. Spina
Investigation: V. Spina
Methodology: V. Spina, J. I. Soto
Project administration: V. Spina
Resources: V. Spina
Software: V. Spina
Supervision: V. Spina, J. I. Soto, J.-C. Ringenbach, S. Mazzoli
Validation: J.-C. Ringenbach, S. Mazzoli
Visualization: J.-C. Ringenbach
Writing – original draft: V. Spina
Writing – review & editing: J. I. Soto, J.-C. Ringenbach, S. Mazzoli

1. Introduction

Large deltas formed on passive continental margins are characterized by gravitational deformation and failure of the thick post-rift sedimentary sequence, which is accommodated by updip basinward extension linked to distal shortening in a deepwater fold–thrust belt (e.g., Allen & Mercier, 1987; Brun & Fort, 2011; Cobbold & Szatmari, 1991; Crans et al., 1980; Crans & Mandl, 1981; Dailly, 1976; Galloway, 1986; Jackson & Galloway, 1984; Morency et al., 2007; Morley, 2003; Winker & Edwards, 1983; Wu et al., 2015). In such delta settings, both extensional and contractional structures commonly detach along weak lithologies such as salt or overpressured shales, which generally flow downslope forming mobile structures (e.g., Hospers, 1971; Ings & Beaumont, 2010; King et al., 2010; Lacoste et al., 2012; Lehner, 1999; Mascle et al., 1973; McClay et al., 1998, 2003; Merki, 1972; Morley & Guerin, 1996; Mourgues & Cobbold, 2006; Mourgues et al., 2009; Rowan, 2020; Tingay et al., 2012; Wu & Bally, 2000; Yuan et al., 2020). In case of gravity spreading, the triggering factors for this structural configuration of the delta margins are the heterogeneous sedimentary load and the weak rheology of salt and shales. In case of gravity gliding, the main parameters controlling basin architecture are the dip variation of the margin slope and thickness variations of the weak layers (e.g., Jackson et al., 1994; Jackson & Hudec, 2017; Maudit et al., 1997; Morley et al., 2011, 2017; Rowan et al., 2004; Vendeville, 2005). General tilting of the margin could be driven by differential thermal subsidence from the continental to the oceanic lithosphere domains, or by regional shortening (due to plate convergence) during an incipient tectonic inversion of the margin (e.g., Hudec et al., 2013, 2020; Rabineau et al., 2014; Soto et al., 2022).

In the specific case of shale-dominated margins, the existence of mobile shale structures and mud volcanoes has been recognized long ago, although it is debated whether these structures are truly diapiric [i.e., piercing; see discussion in Hudec and Soto (2021)]. In this regard, modern 3D seismic data are crucial, as they mitigate issues related to seismic diffractions, noise, and energy loss, enabling a more robust interpretation of mobile shale structures (e.g., Morley, 2003; Morley et al., 2023; Morley & Guerin, 1996; Soto, Hudec, et al., 2021; Van

Rensbergen et al., 1999; Van Rensbergen & Morley, 2003). The Niger Delta is one of the classic margins for which it has been discussed how alternative interpretations of mobile shale structures could impact on the reconstruction of the margin architecture (e.g., Restrepo-Pace, 2020). This is particularly important in estimating the magnitudes of updip extension and deepwater contraction, which may not balance [e.g., see discussions in Butler and Paton (2010), Dean et al. (2015), and Restrepo-Pace (2020)].

In this contribution we use the term mobile shales to describe shale-dominated sequences with a complex combination of brittle and ductile deformation features (e.g., Cohen & McClay, 1996; Hospers, 1971; Merki, 1972; Morley & Guerin, 1996). Mobile shales are capable of flowing and undergo plastic deformation at critical state conditions [first suggested by Brown (1990)]. Under these conditions, complete destruction of the previous sedimentary/deformation fabrics of the shales (i.e., fabric destructuration) occurs, making seismic imaging of mobile shales a challenging task (e.g., Day-Stirrat et al., 2010; Morley et al., 2023; Soto, Heidari, & Hudec, 2021). Processes that help shales becoming mobile include: (a) a high content of organic matter, (b) the abundance of certain clay minerals (particularly smectite), and (c) the existence of overpressure conditions [see review in Soto, Hudec, et al. (2021)]. Overpressure in shales can be induced by processes such as the transformation of organic matter into hydrocarbon fluids, the release of fluids (water) due to diagenetic transformations of clay minerals (e.g., the transformation of smectite to illite), and shortening- or shear-induced overpressure (e.g., Flemings, 2021; Osborne & Swarbrick, 1997; Tingay et al., 2013; Yassir & Addis, 2002). Numerical and experimental models of shale-dominated margins have shown how overpressure conditions evolved over time and spatially within the sedimentary section, also controlling the occurrence of subhorizontal detachments and the generation of fluid escape structures such as mud pipes and mud volcanoes (Albertz et al., 2009; Cobbold et al., 2009; Cobbold & Szatmari, 1991; Ings & Beaumont, 2010; Krueger & Grant, 2011; Morency et al., 2007; Mourgues & Cobbold, 2006; Mourgues et al., 2009).

The present study is dedicated to review the regional configuration and structure of the Niger Delta (Figure 1), where diapiric structures are fed by a thick sequence of overpressured shales (i.e., the Akata Formation; e.g., Maloney et al., 2010; Restrepo-Pace, 2020; Zhang et al., 2021). This margin is also a region of active hydrocarbon exploration and production, and the Akata shales are thought to be part of the source rock layer for hydrocarbons (e.g., Bustin, 1988; Diab et al., 2023; Evamy et al., 1978; Haack et al., 2000; Morgan, 2003; Short & Stäuble, 1967; Stacher, 1995; Tuttle et al., 1999; Whiteman, 1982). We are interested in exploring the following general questions for the Niger Delta, which also have implications for other shale-dominated margins:

1. What is the seismic expression of mobile shales in the delta system? What are the uncertainties in interpreting mobile shales using modern, high-quality 3D seismic data?
2. What is the style and evolution of the deformation, and how are they related to shale mobility in the three structural domains of the delta (i.e., updip extension, "diapiric" region, and deepwater fold–thrust belt)?
3. What role does the lithospheric rifted structure of the margin play in shale mobility?

Answering these questions would provide a better understanding of gravity-driven processes at continental passive margins worldwide, beyond the ongoing debate concerning the styles of deformation characterizing mobile shales in the Niger Delta.

2. Tectonic Setting

2.1. The West African Margin and the Niger Delta

Passive margins result from the progressive thinning and breakup of the continental lithosphere, leading to the formation of new oceanic lithosphere (e.g., Sapin et al., 2012, and references therein). Magma-rich margins (e.g., Geoffroy, 2005) are characterized by up to 20 km thick wedges, which can have Seaward Dipping Reflectors (SDRs) (Hopper et al., 2004; Schreckenberger et al., 2002). SDRs are formed by basaltic flows and sills possibly interbedded with sediments and paleosoils (Sapin et al., 2021). On the other hand, magma-poor margins (e.g., Doré & Lundin, 2015; Sibuet et al., 2004; Sutra & Manatschal, 2012 and references therein) are characterized by limited volumes of syn-rift magmatic rocks and by the exhumation of continental lithospheric mantle at the Continent–Ocean Transition (COT) (Manatschal, 2004; Sapin et al., 2021). Hyperextension is defined as extreme lithospheric stretching that causes crustal faulting reaching into the mantle, triggering its partial hydration or serpentinization (e.g., Manatschal, 2004).

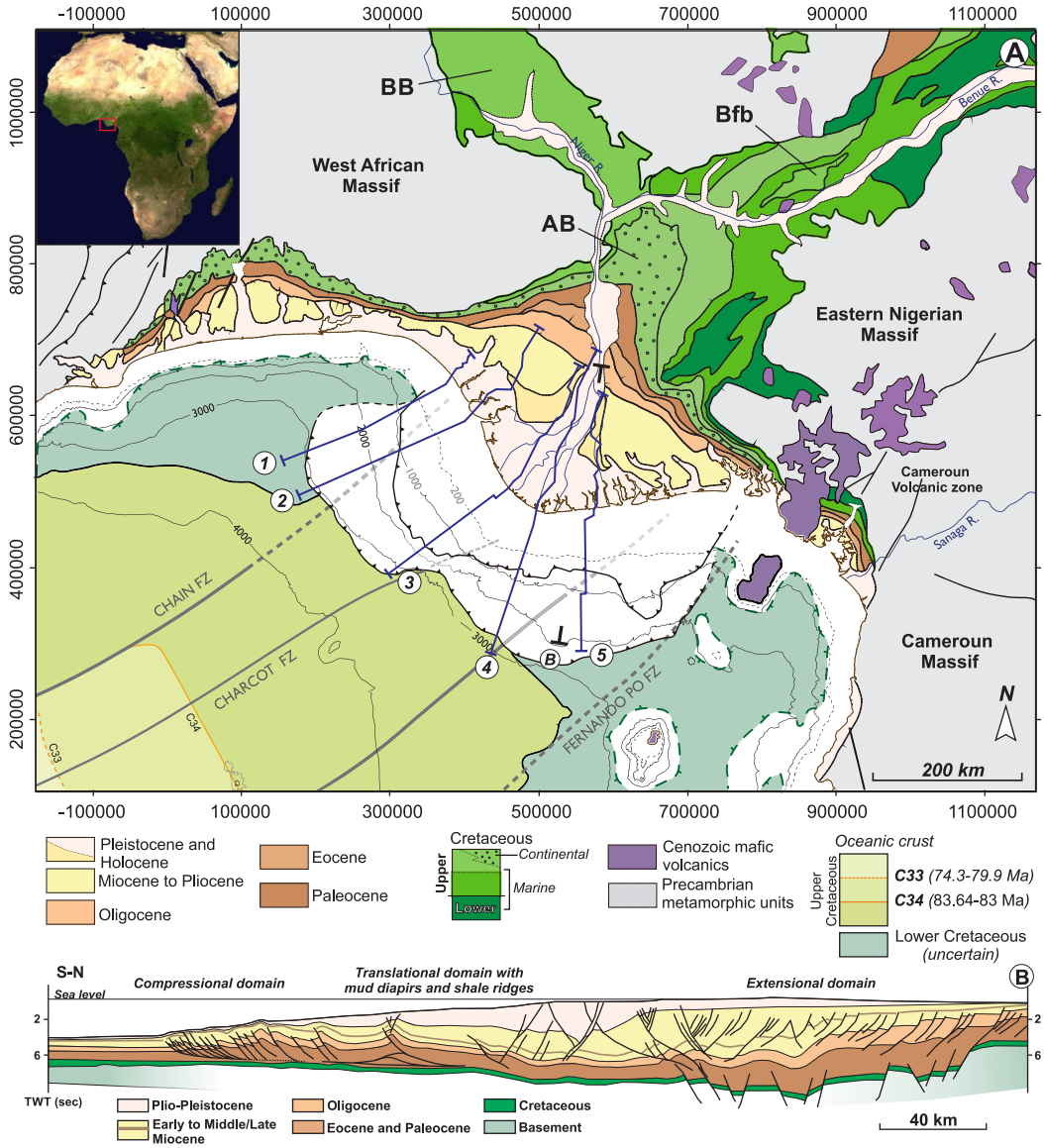

Figure 1. (a) Tectonic map of the Niger Delta region based on our observations and compilation of numerous sources for the onshore region (Adegoke et al., 2017; Ajakaiye & Bally, 2002; Bilotti & Shaw, 2005; Choubert & Faure-Muret, 1990; Evamy et al., 1978; Obaja, 2009; Onuoha, 1999; Reijers et al., 1997; Thiéblemont et al., 2016; Tuttle et al., 1999; Whiteman, 1982) and offshore area (Briggs et al., 2009; Connors et al., 1998; Corredor et al., 2005; Deptuck et al., 2007; Heiniö & Davies, 2006; Krueger & Grant, 2011; Leduc et al., 2012; Wiener et al., 2010). AB: Anambra Basin; BB: Bida Basin; Bfb: Benue fold belt. Magnetic anomalies gridded according to Seton et al. (2020). Magnetic anomalies in the oceanic crust: C33 (74.5 or 74.3–79.9 Ma; Campanian) and C34 anomaly (83.0 or 83.64 Ma; Santonian); ages are according to Cande and Kent (1995) and Ogg (2020), respectively. Oceanic fracture zones (FZ) are after Burke et al. (1971), MacGregor et al. (2003), Samaila and Likkason (2013), Wu et al. (2015), and GEBCO (2024). Bathymetry contour lines (200 m and every 1,000 m) were computed using GEBCO (2023) data set with a grid spacing of 1 arc-minutes (approximately equivalent to 1.8 km). Regional cross sections S1 to S5 are shown in Figure 10. (b) Regional simplified geological cross section (modified from Spina & Mazzoli, 2023) built using available seismic lines illustrating the main structural domains across the entire Niger Delta. Location of the section is shown in panel (a).

The kinematic evolution of the Central African, West African, and Equatorial Atlantic Rift Systems is characterized by a progressive variation of the direction of the regional tectonic extension, leading to a diachronous breakup since the Early Cretaceous (Heine et al., 2013). Brune et al. (2012) suggested that extension oblique to the initial rift axis facilitates rifting and continental breakup. Moreover, transform and highly oblique margins are interpreted

to develop by the reactivation of inherited basement structures (e.g., Mercier de Lépinay et al., 2016) or as newly formed structures linking different segments in the divergent margin (e.g., Le Pourhiet et al., 2017).

The Niger Delta lies at the southern junction of the Benue Trough with the Bida Basin (Figure 1a). These basins are filled by Cretaceous units and lie between the western and the eastern African massifs. Continental drift between African and South American continents and oceanic crust generation started in the Aptian, leading to the progressive opening of the South Atlantic Ocean (e.g., Fairhead & Binks, 1991; Lehner & De Ruiter, 1977; Mascle et al., 1986; Torsvik et al., 2009; Whiteman, 1982). In the offshore domain of the Niger Delta, the Chain, Charcot, Akpo, and Fernando Po oceanic fracture zones are well delineated with seismic and gravimetric data (MacGregor et al., 2003; Samaila & Likkason, 2013; Wu et al., 2015; Figure 1a). Davies et al. (2005), for example, described a series of over 1 km high buried volcanoes along these oceanic fracture zones. Oceanic fracture zones extending from transform faults of the central Atlantic ridge likely influenced the Niger Delta margin, leading to a stepped pre–Cenozoic basement (Figure 1). This, in turn, resulted in a series of parallel SW–NE trending basement highs and lows, associated with Cretaceous depocenters (Cobbold et al., 2009; Evamy et al., 1978; Hooper et al., 2002; MacGregor et al., 2003; Sibuet & Mascle, 1978). However, the role of these faults in controlling the deformation of the Cenozoic delta sediments remains debated (e.g., Spina & Mazzoli, 2023), an issue further explored here.

2.2. Structural Provinces of the Niger Delta

The Niger Delta consists of a large shale-dominated depositional body exposed both onshore and offshore (Figure 1). It underwent Late Eocene to present mixed gliding and progressive gravitational collapse (e.g., Chima et al., 2021; Damuth, 1994; Doust & Omatsola, 1990; Knox & Omatsola, 1989; Rouby et al., 2011).

The structurally controlled deeper portion of the passive margin in the Niger Delta region is overlain by a thick succession of Cenozoic sediments (Chima et al., 2021; Damuth, 1994; Doust & Omatsola, 1990; Knox & Omatsola, 1989; Rouby et al., 2011). The general structure of the delta is well known and is dominated by gravity gliding processes involving a thick and weak sequence of basal shales (the Eocene Akata shales) (Damuth, 1994; Doust & Omatsola, 1990; Knox & Omatsola, 1989). As a result, the delta system developed a wide domain of updip extension and a deepwater contractional fold–thrust belt (FTB). The two are separated by a region traditionally described as the "diapiric province" (Damuth, 1994; Doust & Omatsola, 1990; Knox & Omatsola, 1989). In detail, the deepwater FTB consists of two distinct fold–thrust belts, known as the western and eastern lobes (Figure 1). These lobes partition the delta toe, which spreads over the oceanic Charcot fracture zone (e.g., Briggs et al., 2009; Cobbold et al., 2009; Davies et al., 2005; Wu et al., 2015). The cross section in Figure 1b summarizes the regional structure of the Niger Delta, according to multiple authors (e.g., Chima et al., 2021; Doust & Omatsola, 1990; Zhang et al., 2021).

Corredor et al. (2005) defined several structural domains in the offshore Niger Delta (Figure 1). From north (shallow offshore) to south (deep offshore), these are (a) the updip extensional domain, with basinward (i.e., SW-dipping): listric faults that controlled Eocene to Quaternary sedimentation; in the shallow offshore, these faults are replaced by landward-dipping or counterregional syn-sedimentary normal faults; (b) the so-called mud "diapir" province, located along the present-day continental slope and characterized by active and reactive shale diapirs; (c) the inner fold–thrust belt (FTB), which also involves mobile shales; (d) the transitional domain, dominated by large shale-cored detachment folds; and (e) the outer FTB at the delta toe, with thrusts and fault-related folds trending perpendicular to the regional slope. Contraction in the deepwater FTB began around 15 Ma, peaked between 9 and 3.5 Ma, and is still active today, as indicated by seafloor deformation (e.g., Higgins et al., 2009; Jolly et al., 2016; Krueger & Grant, 2011; Pizzi et al., 2020; Spina & Mazzoli, 2023; Sun & Liu, 2018).

3. Lithostratigraphy

The Niger Delta contains a ∼12 km thick sedimentary succession, including subaerial fluvial delta deposits and deep-water slope to basin-floor sediments (Burke, 1972; Burke et al., 1971; Chima et al., 2019; Damuth, 1994; Doust & Omatsola, 1990; Evamy et al., 1978). The present-day delta results from ∼300 km of downslope (southward) translation of the delta front, accompanied by sedimentary progradation and gravity-driven deformation (Bilotti & Shaw, 2005; Briggs et al., 2006; Evamy et al., 1978; Morgan, 2003; Rouby et al., 2011).

The sedimentary infill of the Niger Delta overlies oceanic crust and highly stretched continental crust associated with the rifted margin (Figure 1) (e.g., Burke, 1972; Burke et al., 1971; Corredor et al., 2005; Ekweozor & Daukoru, 1994). The Cretaceous section, roughly coeval with continental break-up, remains of uncertain composition and thickness offshore due to the lack of well penetration. Onshore, in the Anambra Basin, this sequence consists of shallow-marine clastic units (Figure 1a) (e.g., Ajakaiye & Bally, 2002; Onuoha, 1999; Reijers et al., 1997; Short & Stäuble, 1967; Thiéblemont et al., 2016).

Throughout the entire Niger Delta, the Cenozoic succession is subdivided into three major units (from bottom to top; Figure 2): the Akata Formation, the Agbada Formation, and the Benin Formation (Adegoke et al., 2017; Avbovbo, 1978; Doust & Omatsola, 1990; Evamy et al., 1978; Knox & Omatsola, 1989; Short & Stäuble, 1967; Tuttle et al., 1999; Whiteman, 1982). The Akata Formation is interpreted to date from the Paleocene to Recent (Avbovbo, 1978; Doust & Omatsola, 1990; Haack et al., 2000), although in the distal offshore region it has been assigned a Middle–Upper Eocene to Oligocene age (e.g., Ekweozor & Daukoru, 1994). This unit mainly consists of marine shales with significant thickness variations, ranging from 2 km in the most distal part of the delta to 7 km beneath the continental shelf (e.g., Doust & Omatsola, 1990). In the deepwater domain, basin floor fans, debris flows, deepwater channel complexes and shales of the Agbada Formation overlie the Akata Formation (Avbovbo, 1978; Doust & Omatsola, 1990; Haack et al., 2000; Krueger & Grant, 2011).

The Agdaba Formation includes an up to 3.5 km thick clastic succession deposited in various sedimentary environments, such as the delta front, the delta top, and a mixed fluvio-deltaic setting (e.g., Ogbe, 2020). Coarse-grained deposits within this succession interfinger with several clay-rich levels (i.e., the Boguma, Soku, and Afam clays; Figure 2). Onshore and in the updip extensional domain of the Niger Delta, the Benin Formation overlies the Agbada Formation, which consists of fluvial sands of Oligocene to Recent age (Avbovbo, 1978; Ogbe, 2020; Short & Stäuble, 1967).

The Akata Formation is widely recognized as the primary source rock for hydrocarbons in the basin, while the overlying Agbada Formation hosts multiple reservoir intervals (e.g., Doust & Omatsola, 1990; Ekweozor & Daukoru, 1994).

3.1. Seismic Facies and Overpressure of the Akata Formation

Various authors (Briggs et al., 2006; Cobbold et al., 2009; Higgins et al., 2009; Maloney et al., 2010; Zhang et al., 2021) proposed that the Akata Formation contains multiple regional detachments imaged as high–amplitude seismic reflections, known as the X, Y, and Z reflectors (see seismic panel for the toe of the delta in Figure 2). Reflector X marks a level near the stratigraphic boundary between the Agbada and Akata formations. Regionally, it is situated at approximately 6.8 s two-way travel time (TWT) in the western lobe of the delta and at about 5 s TWT in southernmost sector of the eastern lobe (Corredor et al., 2005; Maloney et al., 2010; Zhang et al., 2021).

Reflector Y, commonly referred to as the mid–Akata detachment, defines the base of the Upper Akata. This strong reflector appears as a package of discontinuous, low-amplitude seismic reflections (e.g., Maloney et al., 2010; Zhang et al., 2021). In the western lobe, this reflector is situated at about 7 s TWT, whereas in the southernmost sector of the eastern lobe, it is observed between 6.5 and 5.5 s TWT (e.g., Maloney et al., 2010; Zhang et al., 2021).

The lowermost seismic event is a high-amplitude seismic package, known as the Z reflector, which marks the base of the Paleocene series (the Pre-Akata Sedimentary Wedge or PASW; *sensu* Briggs et al., 2006). In the northern sector of the deepwater domain, this reflector appears as a high–amplitude, faulted reflector at about 8.8 s TWT and is interpreted as the top of the acoustic basement (Maloney et al., 2010). In the southernmost sector of the eastern lobe, the Z reflector is shallower, lying at approximately 6.9 s TWT. Despite the regional description of its seismic expression, the precise lithology and age of the Akata Formation remain uncertain due to the lack of wells fully penetrating this unit.

The shales of the Akata Formation are characterized by undercompaction and overpressure conditions due to high sedimentation rates and rapid delta progradation (Cobbold et al., 2009; Krueger & Grant, 2011; Morgan, 2003; Swarbrick et al., 2011). These factors, along with their low densities (typically $2.3–2.4 \times 10^3$ kg/m^3), influence their mechanical behavior (e.g., Jacques et al., 2003; Nwozor et al., 2017).

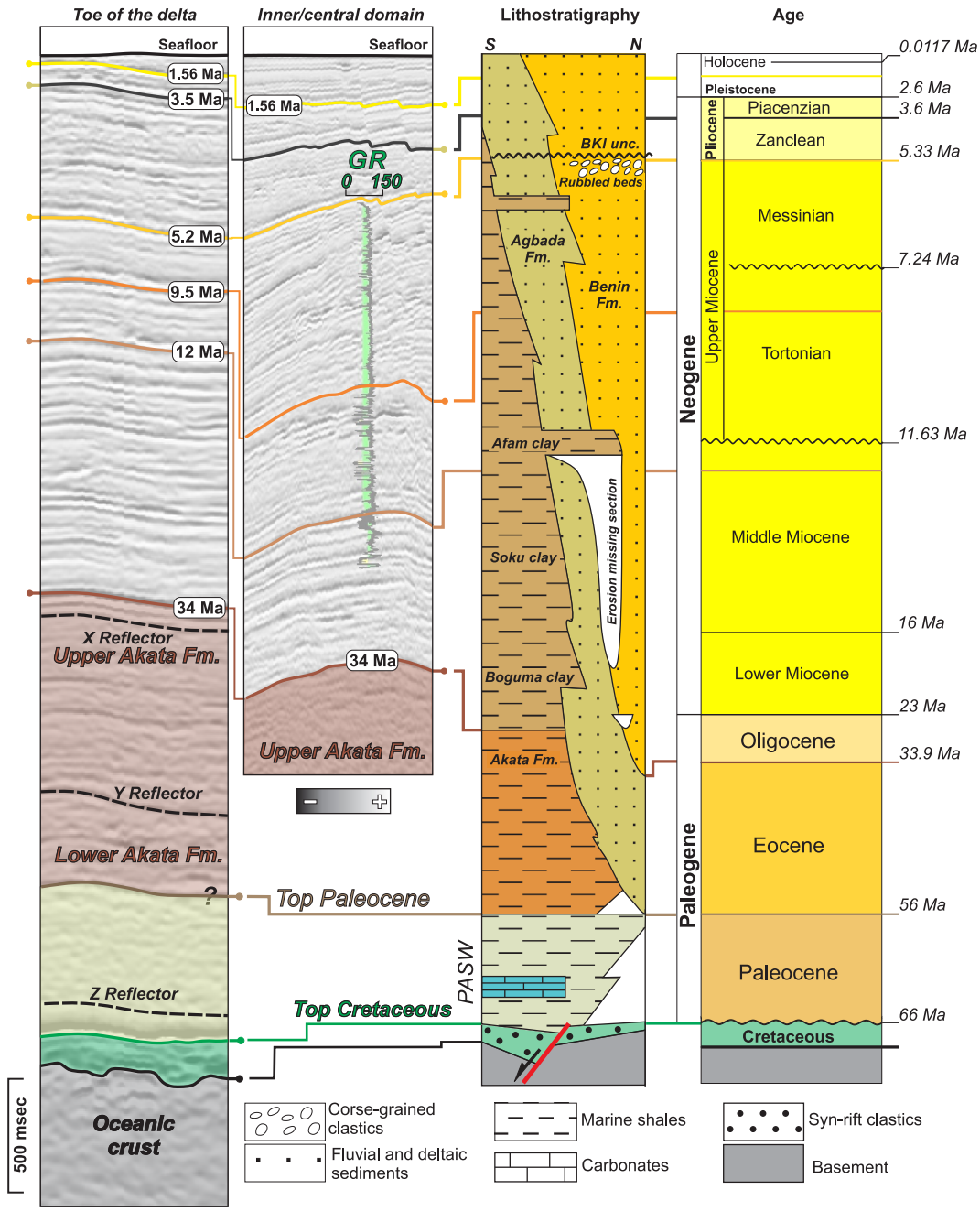

Figure 2. Chronostratigraphic summary columns for the Niger Delta. The panel integrates industry data made available to us and multiple sources (e.g., Adegoke et al., 2017; Doust & Omatsola, 1990; Reijers et al., 1997; Tuttle et al., 1999). The stratigraphic position, age, and seismic character of the regional seismic discontinuities used in this study are marked in the different columns. PASW is for Pre-Akata Sedimentary Wedge (*sensu* Briggs et al., 2006).

4. Data Set and Methods

This study is based on over 500,000 km of 2D seismic lines of varying resolution and vintage, with frequencies between 5 and 30 Hz (vertical resolution of 30–10 ms TWT). In addition, multiple 3D seismic data sets (7–44 Hz) covering the onshore and shallow offshore domains were interpreted. A selection of these data sets is shown in Figure 3 and Figures S1 to S5 in Supporting Information S1. Seismic data were provided by TotalEnergies, Shell, PSG, and TGS.

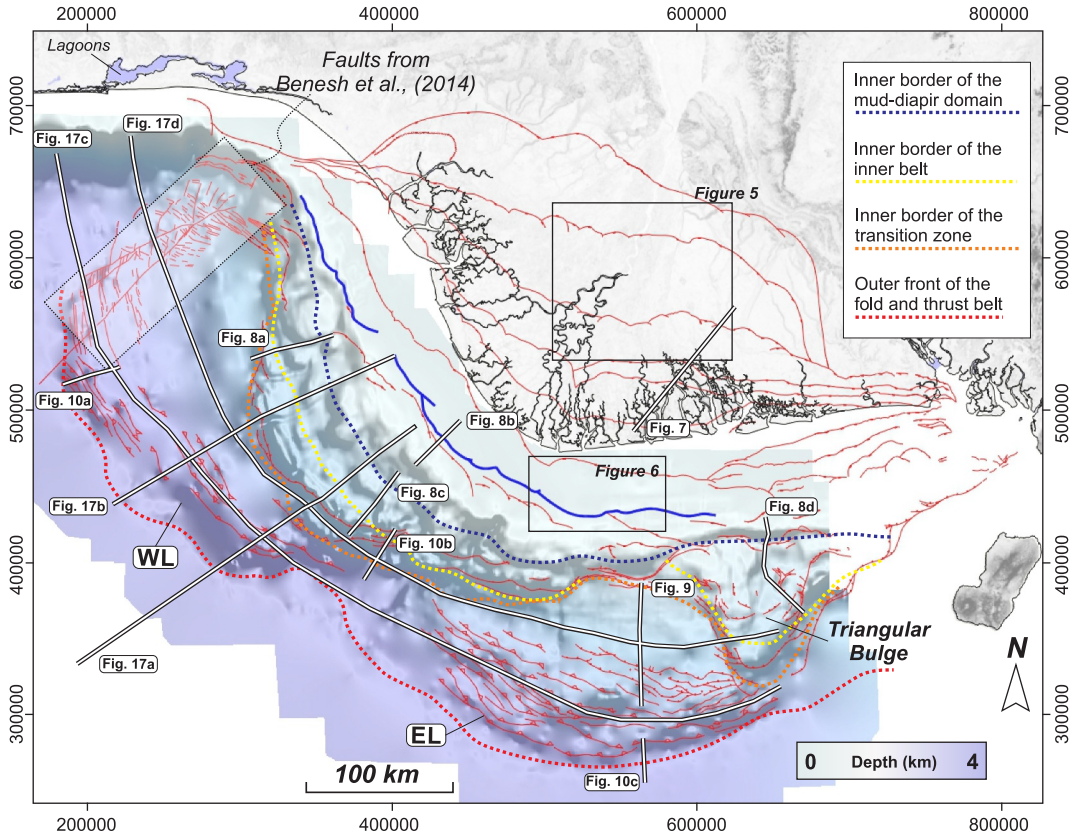

Figure 3. Regional structural map of the Niger Delta overlain onto a bathymetry map (derived from the seismic data set), showing location of the seismic lines of Figures 5–9, 17, and 18. Red lines correspond to the main faults (including local observations from Benesh et al., 2014); blue lines correspond to the landward-dipping ("counterregional") faults. EL: Eastern Lobe; WL: Western Lobe. Dashed lines show the limits of the structural domains identified by Corredor et al. (2005), mapped at the seabed.

Key regional seismic markers were correlated using well data (Figure 2). Age constraints were established through nannofossils, foraminifera, and palynology analyses, which were integrated with well logs to refine seismic interpretation. This approach allowed us to identify and map major seismic discontinuities at 1.56 Ma (Lower Pleistocene), 3.5 Ma (Upper Pliocene), 5.2 Ma (Lower Pliocene), 9.5 Ma (Tortonian, Upper Miocene), 12.0 Ma (near base of Tortonian), and 34 Ma (top Eocene) (Figure 2). In many areas, the 34 Ma reflector marks the top of the mobile shale unit.

Seismic interpretation was performed in time domain and complemented with isochore maps (stratigraphic thickness in TWT). These maps were derived from gridded surfaces using dip and azimuth to avoid overestimating time thickness, especially in high-dip areas. We built five regional seismic lines covering the entire Niger Delta (Figure 1). These lines were depth-converted using well log data and published time–depth relationships (e.g., Chima et al., 2021).

Restoration was performed using Move Suite software (©Petroleum Expert). Line–length balancing and progressive decompaction were applied, assuming vertical subsidence and using average decompaction curves. No corrections were made for global sea–level variations. Fault displacement was restored with the Move-on-Fault tool, testing the Fault–Parallel Flow algorithm for better geometric reconstruction. Folds were restored using the Unfold tool with different algorithms. Vertical Shear was used for faulted units, Flexural-slip for the FTB (Carboni et al., 2018; Ogawa & Back, 2022), and Vertical Shear for the mobile-shale structures (Rowan & Ratliff, 2012). These restorations assume: (a) plane strain, (b) no internal strain, and (c) no volume change during deformation. While 3D flow in Niger Delta shales is documented (e.g., Spina & Mazzoli, 2023), 2D restorations remain a valid first approximation for regional studies (e.g., Rowan & Ratliff, 2012). Internal strain and volume

changes can be significant, particularly in shale-dominated systems (e.g., Butler & Paton, 2010). As a result, the estimated horizontal shortening in the Agbada and Akata Formations represents a minimum value.

5. Seismic Interpretation of Mobile Shales

Shale properties influence their seismic expression due to factors like composition, fluid content, thermal conditions, and deformation history (Day-Stirrat et al., 2010; Morley et al., 2008, 2011, 2017; Soto, Hudec, et al., 2021). The Akata Formation appears in seismic profiles as a thick, acoustically transparent package. However, near the basin margin and in deep offshore, it displays subparallel, high–amplitude reflectors with increasing frequency toward the bottom (Figure 2). Seismic velocities in the Akata Formation are generally low (2,000–3,000 m/s, mean 2,600 m/s; Cobbold et al., 2009; Maloney et al., 2010; Morgan, 2003) and increase downward at low gradient (0.2 s/km). These values are up to 30% lower than those of the overlying Agbada Formation (Cobbold et al., 2009).

Soto, Hudec, et al. (2021) reviewed the seismic characteristics of mobile shales. Despite the lower resolution of the 2D seismic data set used here, we conducted a detailed interpretation of the mobile–shale structures and nearby units (Figure 4). Key observations include: (a) gradual contacts with supra-shale sequences (Figures 4a–4d), (b) challenges in imaging pre-shale sequences and defining shales base (Figures 4a and 4b), and (c) common seismic artifacts like diffractions and internal noise (Figures 4b and 4d). In some cases, lateral wings in the roof sequences or subvertical contacts in mud pipes add complexity to the interpretation (e.g., Figure 4d).

The top of mobile shales likely coincides to the Eocene–Oligocene boundary (dated at 34 Ma; Figure 2). In less deformed regions, like at the delta toe, this contact appears as a strong and continuous negative reflection (Figure 2). However, in areas where the mobility of the shales is more important the interpretation of their top is less certain (Figure 4). In these sectors, the mobile shales are generally characterized by a sharp downward decrease in seismic reflectivity. They have transparent and chaotic seismic facies, with occasional strong planar reflections, likely remnants of shale bedding or preserved intra-shale lithologies (Figures 4b and 4d).

The base of mobile shales is defined by discontinuous, high-amplitude reflections but is affected by seismic artifacts like smiles and push–down effects, related to low velocities and processing limitations (e.g., Morley, 2003; Morley et al., 2017; Morley & Guerin, 1996; Soto, Hudec, et al., 2021; Spina & Mazzoli, 2023; Zhang et al., 2021). Some seismic lines show supra-shale sequences directly overlying pre-shale units, interpreted as a primary shale weld due to the complete shale evacuation (Figure 4b). This welding produces the direct superposition of supra-shale series (Oligocene and younger) onto pre-shale ones (of Paleocene and Cretaceous age) and even on top of basement highs.

Active normal faults detach above shale ridges, forming rollovers, while mobile shales create triangular footwall bodies resembling shale rollers (Figures 4a and 4b). These triangular bodies, or shale ridges, have been previously described by many authors in the area (e.g., Evamy et al., 1978). Some minibasins contain double-wedge geometries with internal discontinuities and onlaps, resembling salt-related minibasins (Figure 4c). Their complex architecture suggests progressive shale evacuation and flow, similar to salt systems (e.g., Jackson & Hudec, 2017).

In the Niger Delta, mobile shales form broad highs or shale walls, feeding detachment anticlines and fault–related folds (e.g., Connors et al., 1998; Corredor et al., 2005; Heiniö & Davies, 2006; Spina & Mazzoli, 2023). These elongated structures extend up to 20 km, with changes in vergence (e.g., Pizzi et al., 2020). Shale diapirs and walls can reach 8 km in height, with feeder systems exceeding 3 km in diameter (Morley, 2003; Morley & Guerin, 1996). Many shale diapirs are associated with small planar normal faults at their crests, forming collapse-related grabens that deform the roof series up to the seafloor (e.g., Corredor et al., 2005). Further evidence of shale mobilization and fluid expulsion in anticline culminations includes subvertical mud pipes with stacked shale wings and active mud volcanoes (Ajakaiye & Bally, 2002; Benjamin & Huuse, 2017; Dupuis et al., 2019; Graue, 2000; Morley, 2003). These structures, described as shale "chambers" (*sensu* Morley & Guerin, 1996), indicate repeated pulses of mobilization (e.g., Dupuis et al., 2019). These mud volcanoes extrude Pliocene and possibly Upper Miocene material (*extrusiva*; *sensu* Kopf, 2002) and also occur in the onshore extensional domain, in the Anambra Basin and in the Benue Trough (Musa et al., 2014, 2016).

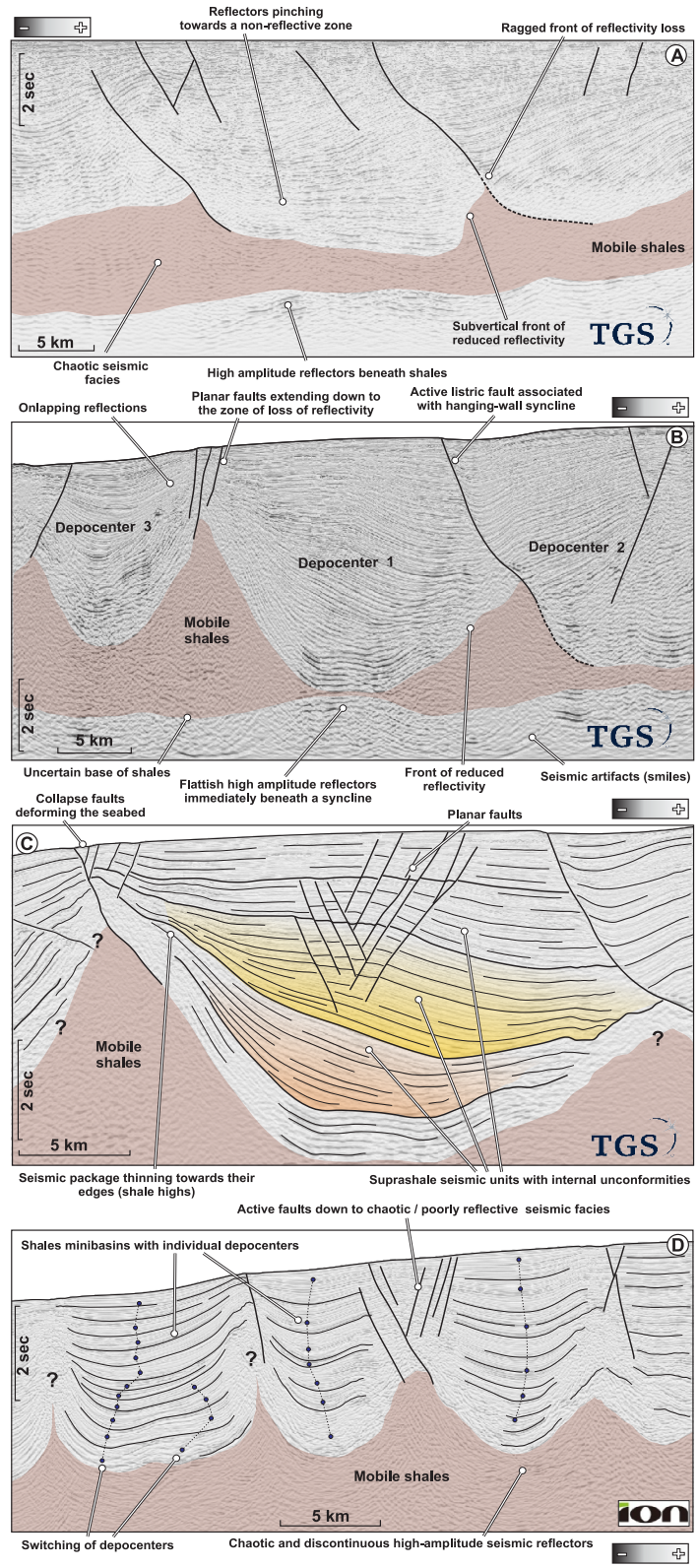

Figure 4. Seismic examples of mobile shales and associated structures, showing the criteria used for seismic interpretation and associated uncertainties.

6. Structural Styles in the Niger Delta

This section describes the structural styles and timing of the deformation for the regional domains of the Niger Delta, from the onshore area to the deepwater domain (Figures 1 and 3).

6.1. Updip Extensional Domain

The updip extensional domain of the Niger Delta is characterized by growth faults that affect both the present-day onshore and shallow offshore regions (Figures 1b and 3). These normal growth faults create narrow, elongated depocenters associated with Eocene–Pleistocene sediments, representing the initial stage of delta progradation (Chima et al., 2021; Cohen & McClay, 1996; Wiener et al., 2010).

6.1.1. Onshore Sector

In the onshore sector, seismic data reveal a dense network of south-dipping normal fault segments (Figure 5). These faults offset basinward-thickening sequences bounded by south-dipping seismic reflections. In map view, the segments are ∼10 km long and concave toward the southwest (Figure 5a), consistent with local descriptions (Amogu et al., 2011; Ekweozor & Daukoru, 1994; Magbagbeola & Willis, 2007; Sanuade et al., 2018). Their geometry suggests listric faulting, likely detaching within the Akata Formation.

At ∼4 s TWT depth, the shales show no evidence of large diapirs. Wedges and growth strata are observed within the Eocene units in the hanging wall of extensional faults (Figures 5b and 5c). Based on seismic resolution, Middle–Upper Miocene sediments appear post-kinematic, as indicated by an unfaulted reflector dated to 12 Ma (Figures 5b and 5c). Moreover, minor sub-seismic faults, such as small reactivation or compactional faults, could exist at the upper tips of major structures, possibly affecting younger sediments. These observations suggest that onshore normal faulting initiated during the Eocene and ceased in the Lower Miocene.

6.1.2. Shallow Offshore Sector

In the shallow offshore sector, where the delta extends beyond the continental edge, the structural architecture is dominated by extensional faults striking perpendicular to the regional slope (Figure 6). A 3D seismic data set from this area reveals a folded package of seismic reflections underlain by a poorly reflective package, interpreted as mobile shales (filled in brown in Figure 6).

Time slices show that these poorly reflective domains cut across the seismic layering of the overlying sequences (Figures 6a–6c), forming geometries similar to minibasins in salt systems (Figure 6d). A radial pattern of extensional faults is observed around the shale crests (Figures 6b and 6c), with some extensional faults detaching at the transition between layered sequences and chaotic seismic domains (Figure 6d). Further extensional faults, striking mainly E–W (Figures 6a–6c), cluster around the structural culmination and are slightly oblique to the shale high trend.

Previous studies described these offshore listric faults as merging along a gently dipping sequence of Akata shales (e.g., Maloney et al., 2010). Below the normal faults, seismic artifacts such as smiles and multiples, along with a sharp reduction in seismic layering, make it difficult to trace their depth continuation as growth faults (e.g., Figure 6d).

In the domains with mobile shales, the wedge geometries of the roof sequences help constrain fault structures. These shale minibasins consists of asymmetric wedges that thicken northward and against the shale highs, suggesting the occurrence of counterregional normal faults or mobile shale flow (Figure 6d).

In the offshore domain, the top of the overpressure zone is estimated at approximately 4–5 km in the continental shelf and at 2.3–2.5 km in the deepwater region (Cobbold et al., 2009; Krueger & Grant, 2011; Morley, 2003; Swarbrick et al., 2011). The rapid burial has led to a relatively constant pressure gradient (0.0105 MPa/m), allowing the preservation of high pore-fluid content in these shales (e.g., Krueger & Grant, 2011). The pore-fluid pressure ratio (λ) in this succession is estimated to reach values as high as 0.9 (*sensu* Bilotti & Shaw, 2005). Toward the continent, the top of the overpressure zone progressively truncates older successions (Figure 7). This basinward younging of the overpressure top is commonly observed in deltas with thick accumulations of clastic sediments (e.g., Chapman, 1994; Harkins & Baugher, 1968).

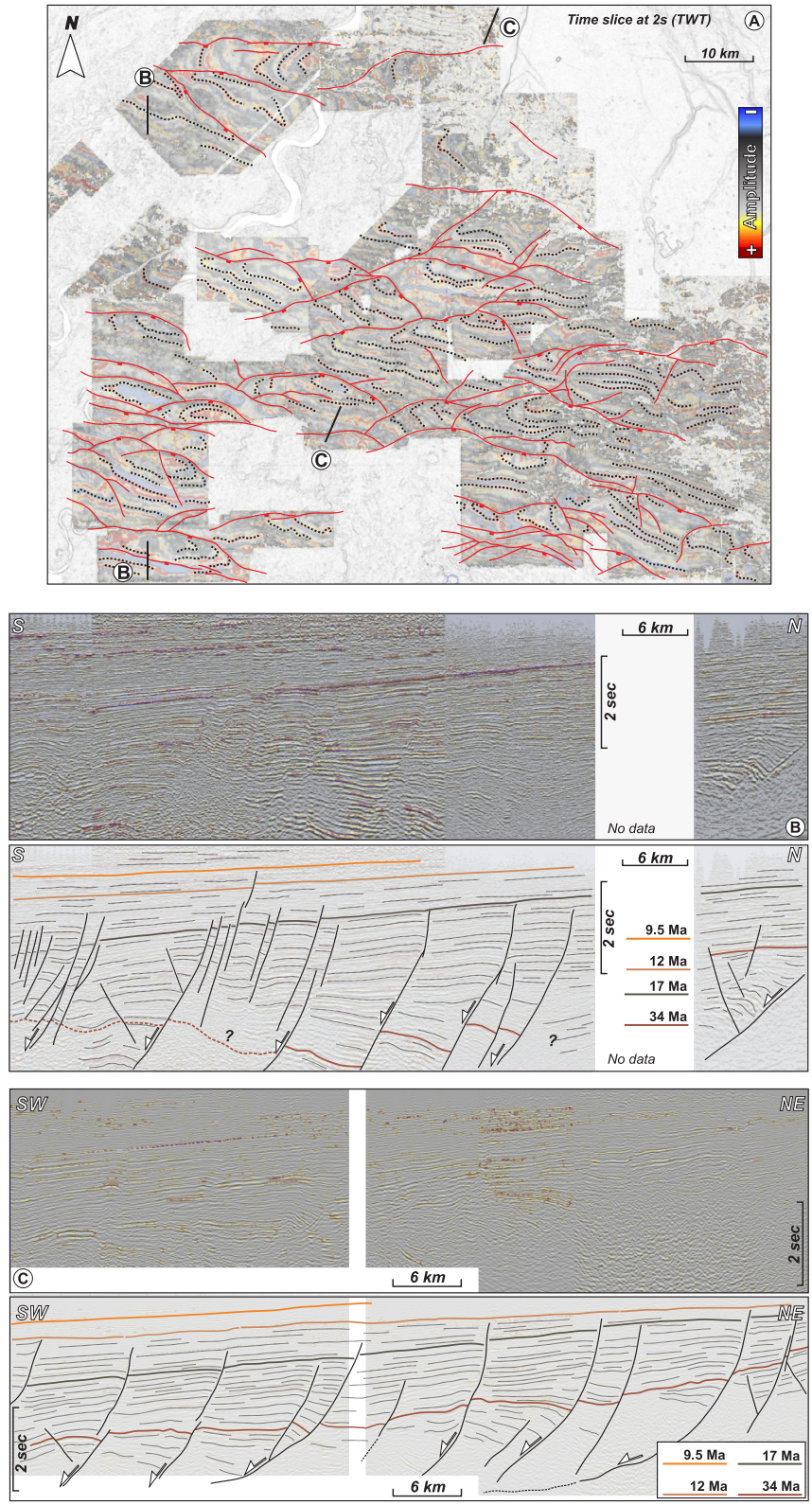

Figure 5. Structural architecture of the onshore domain of the Niger Delta obtained by interpretation of a seismic volume. (a) Time slice at 2 s two-way travel time (TWT) overlain on a greyscale digital topography for reference (NOAA, 2022). (b)–(c) Two arbitrary seismic sections and their interpretation showing the geometry of the normal faults and the age of the main geological discontinuities. Location of (b) and (c) is marked in (a). General location of this area is shown in Figure 3.

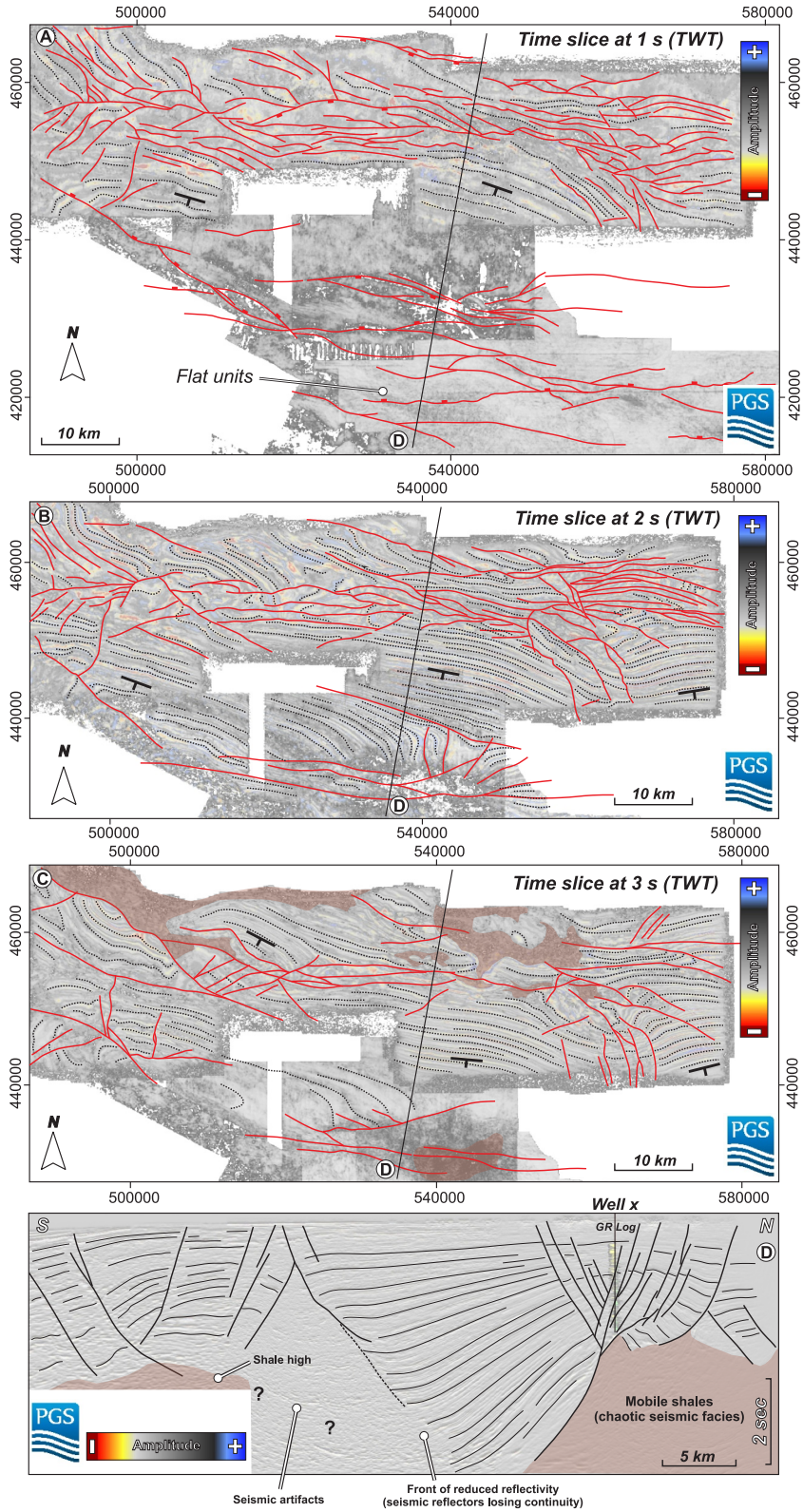

Figure 6. Structural architecture in the shallow offshore domain of the Niger Delta obtained by interpretation of a seismic cube. (a) Time slice at 1 s (TWT), (b) time slice at 2 s TWT, (c) time slice at 3 s TWT, and (d) SSW–NNE arbitrary seismic line with interpretation. Location of (d) is marked in (a) to (c). General location of the area is shown in Figure 3.

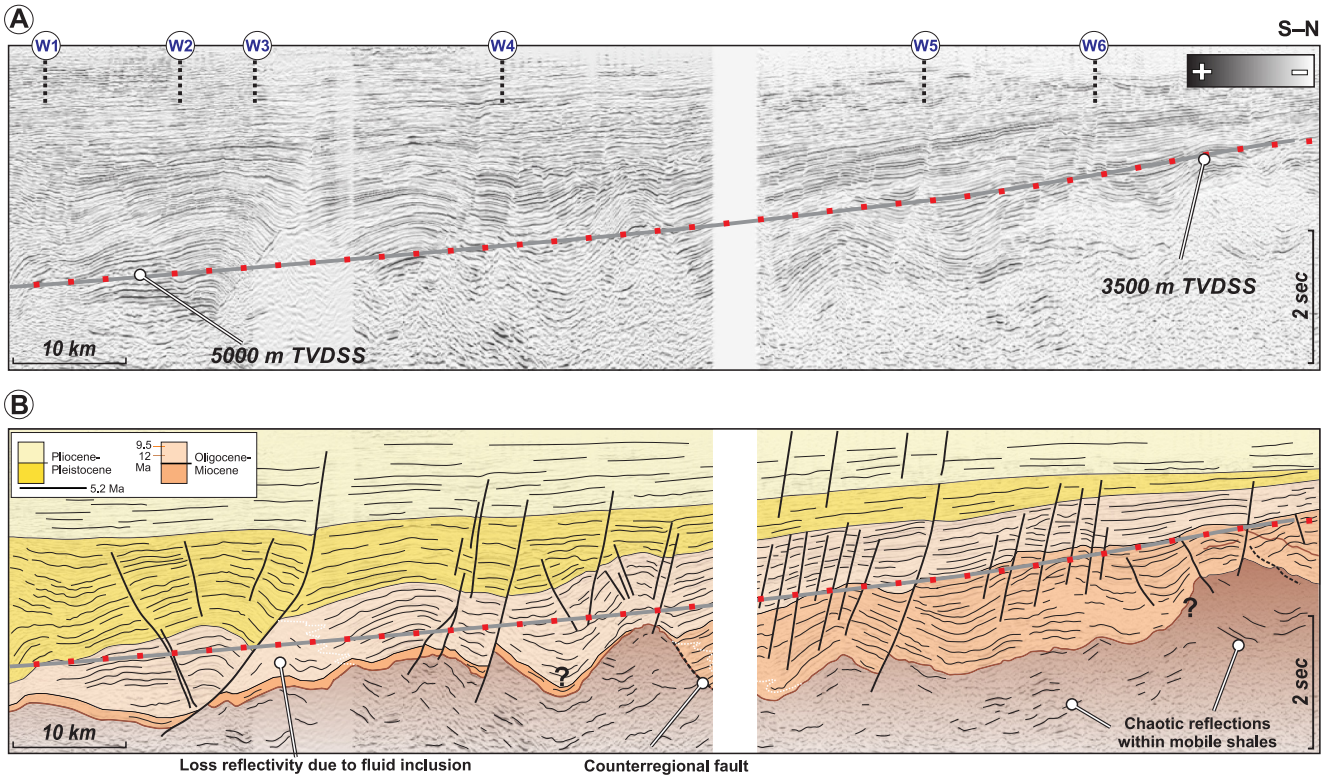

Figure 7. Uninterpreted seismic line (a) and interpretation (b) illustrating the progradation of the delta in the onshore domain. See location in Figure 3. Delta prograding wedges were deposited over mobile shales and progressively subsided, leading to lateral expulsion of the shales. Shale flow is interpreted to create accommodation space occupied by the next generation of delta. Borehole data (projected along the line) were used to calibrate the present-day position of the top of overpressure surface. The overpressure front dips southward and cuts across the stratigraphy.

6.2. "Diapiric" Domain

The mud "diapir" province (Corredor et al., 2005) extends along the continental slope of the entire delta, including the western and eastern lobes (Figures 1 and 3). This 20–30 km wide zone is characterized by significant mobility of both Akata and Paleocene shales (Figure 8). Shale mobility is evidenced by shale pillows, shale-cored anticlines, tall shale walls (Figures 8a–8c), isolated diapirs (Figure 8a), subvertical mud pipes with small lateral wings (Figure 8c), and mud volcanoes (e.g., Graue, 2000).

Piercing shale diapirs, walls, and ridges are covered by thinner, gently deformed roof sequences. In some cases, these sequences are overlain directly by the seafloor, with symmetrical crestal collapse faults or asymmetric basinward and counterregional crestal growth faults (Figures 8a, 8b, and 8d). Depocenters around the mobile-shale highs contain post-Eocene sediments exceeding 4 s TWT in thickness (Figure 8). These units thicken toward the center of each flanking depocenter and thin centrifugally over the shale highs, where they may be eroded.

In the Triangular Bulge of the delta (Figures 1a, 3, and 8d), Pliocene sediments unconformably overlie Upper Miocene sequences, likely deformed by shale flow (see also Oguadinma et al., 2024). Seismic data show that this unconformity, the BKI unconformity, is occasionally associated with reddish continental conglomerates known as the "Rubbled beds" (Figure 2). Above the mobile shale highs, this surface is gently deformed.

We interpret that shale mobility in this domain began during the Miocene and continues to the present. At the continental edge and along the slope, persistent and active shale movement has controlled sedimentation since the Miocene. Oligocene–Recent sediments have accumulated in subsiding troughs around mobile shale highs. In some areas, the base of the lowermost post-shale sequence (Oligocene to Middle Miocene) lies directly on high-amplitude reflections interpreted as bedrock (Figures 8c and 8d). This geometry suggests a primary shale weld, where the mobile unit was completely removed and evacuated laterally.

10.1029/2024TC008689

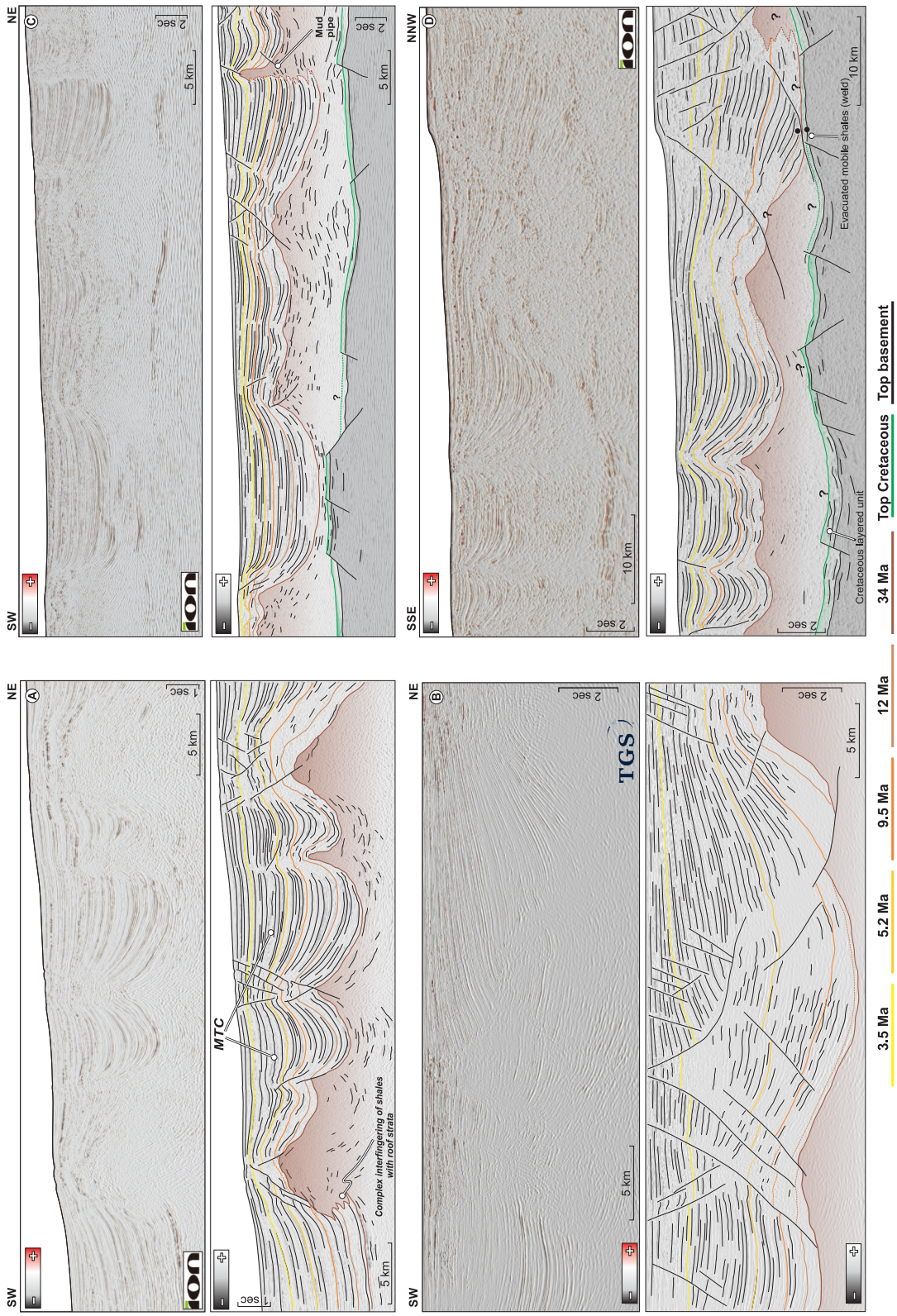

Figure 8. (a–d) Seismic examples of mobile shales in the "diapiric" domain and associated tectonic structures. See location in Figure 3. The pseudo-relief filter applied to the seismic lines enhances contrast and emphasizes the continuity of seismic reflections. Uninterpreted, higher-resolution versions of (a) and (b) are provided in Figure S1 in Supporting Information S1. MTC: mass-transport complex.

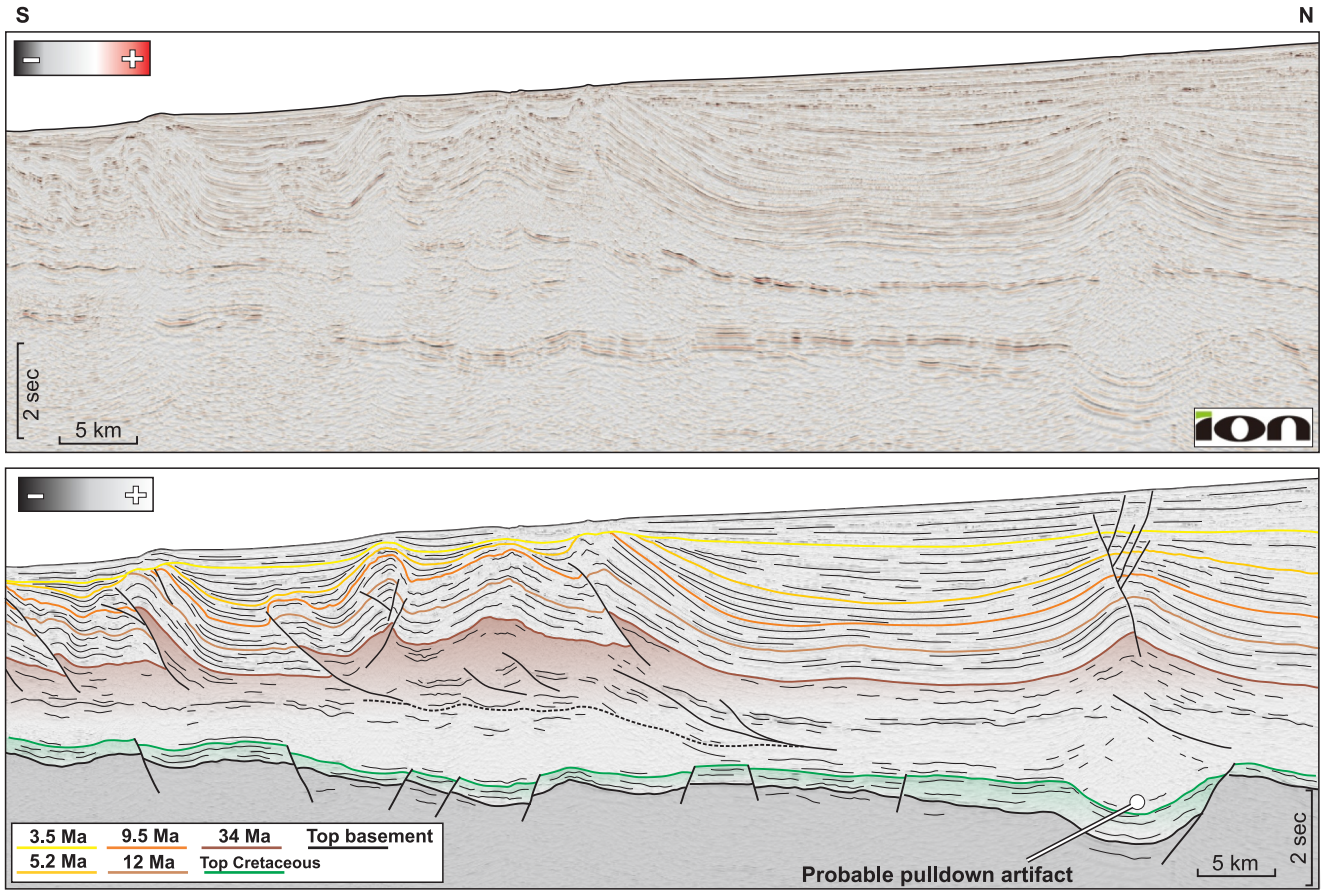

Figure 9. Seismic section showing the transition from tight folds in the "diapiric zone" of the delta to the deepwater fold–thrust belt involving mobile shales. See location in Figure 3. The pseudo-relief filter applied to the seismic lines enhances contrast and emphasizes the continuity of seismic reflections. Uninterpreted, higher-resolution version of the seismic line is provided in Figure S2 in Supporting Information S1.

The NW–SE oriented shale highs and their arched roofs appear have undergone contractional deformation, possibly linked to active shale diapirism [see Rowan and Giles (2021) for a discussion on this terminology]. These structures characterize the so-called inner FTB, mapped along both western and eastern lobes by Corredor et al. (2005) (Figure 3). However, contractional deformation around mobile shale highs is more prominent in the western lobe, narrowing toward the Charcot fracture zone (Figure 3).

Within the inner FTB, mobile shales form elongated highs and walls, associated with thrust faults that, in some cases, overthrust mobile shales onto Oligocene–Middle Miocene sediments (Figure 8a). Similar contractional deformation is also recognized in the Triangular Bulge, at the termination of the eastern lobe (Figures 3 and 8d).

The transitional zone (*sensu* Corredor et al., 2005) coincides with two large embayments within the western and eastern lobes (Figure 3). This domain contains large detachment anticlines fed by inflated mobile shales. These folds deform an isopachous package of low-reflective, layered seismic units corresponding to the Agbada Formation (Figure 9). Pre-shortening sequences in these anticlines are typically pre-Tortonian (below the 9.5 Ma reflector). Overlying sequences, up to the seafloor, show onlaps and truncations. These observations indicate that shortening in this sector mainly occurred post-9.5 Ma (Tortonian and younger). The timing of deformation aligns with studies from other areas of the Niger Delta (Chima et al., 2021; Pizzi et al., 2020; Spina & Mazzoli, 2023).

6.3. Deepwater Contractional Domain

The outer FTB (*sensu* Corredor et al., 2005) corresponds to the toe of the Niger Delta (Figure 1), forming a narrow zone of thrust-related folds. Figure 9 illustrates the transition from the "diapiric" zone to the deepwater FTB, where structures evolve from symmetric shale ridges and detachment folds to basinward-verging thrust-related

anticlines. In the deepwater FTB, these thrusts detach within the Akata Formation, where they merge along some reflective layers, and their upper fault tips are located within Miocene sequences (between the 12 and 9.5 Ma reflectors). These shales accommodate thrusting through lateral flow, promoting fold growth (Figure 9).

Figures 9 and 10 show the structural variability across three sectors of the deepwater FTB (location in Figure 3). In the western lobe, narrow basinward-dipping thrusts detach within a poorly reflective seismic package (Figure 9a). Thrust dip direction shifts to landward-dipping over a short distance southwestward, deforming an almost isopachous package of Oligocene–Miocene units (Figure 10a). These changes in thrust dip direction have been previously described and interpreted as associated with the presence of tear faults compartmentalizing the thrust system (e.g., Benesh et al., 2014). Progressive unconformities and thickness variations within the Pliocene–Pleistocene units suggest they were deposited during fold growth, with active deformation reaching the seabed (Figures 10a and 10c). Thrust dip direction variability and associated fold geometry (Figures 9 and 10) reflect buckling controlled by rheological contrasts between weak mobile shales and more competent post-Eocene sediments.

At the Charcot fracture zone, where the western and eastern lobes merge, steep, south-verging thrusts deform an isopach Miocene–Pliocene seismic package (between the top Eocene and 5.2 Ma reflectors) (Figure 10b). These thrusts, active during the Early Pliocene, are sealed by the 3.5 Ma reflector. In the easternmost section of the seismic line shown in Figure 10b, the Akata shales form a structural high that resembles an asymmetric diapir affected by later shortening. Thrusts from this structure propagate upward, deforming Pliocene–Pleistocene sediments and the seabed (Figure 10b).

Closely spaced folds associated with north-dipping thrusts are also imaged along the eastern lobe of the Niger Delta (Figure 10c). These structures deform an almost isopachous seismic package of sediments older than the 9.5 Ma reflector (pre-shortening units). Thrusts detach beneath a continuous, high-amplitude reflector within the Akata shales, exhibiting listric geometries with steep ramps (approximately 50°, Figure 9c). Although not always visible in seismic data, we suggest these faults merge within the Akata shales, which behaves as a weak, detached layer potentially containing multiple sub-horizontal detachments and duplexes.

A further notable feature in Figure 10c is the superposition of short-wavelength imbricate folds over broader, long-wavelength folds. This may result from the activation of different detachments or minor reactivation (inversion) of deep-seated inherited faults affecting the basement (Figure 10c) [as was also suggested by Morgan (2003) and Spina and Mazzoli (2023)]. In this sector of the deepwater FTB, the intra-Akata detachment is approximately 1 s TWT shallower than in the western lobe (cf. Figures 10a–10c), deepening northward into the transition zone. There, seismic data indicate intense deformation within the Akata shales (Figure 9). Deformed Upper Pliocene sediments (post-3.5 Ma) unconformably cover and onlap the underlying units, indicating that contractional deformation began primarily during the Early Pliocene and remains active today, as evidenced by the deformed seafloor (Figure 10c).

7. Regional Structure of the Niger Delta

Five SW–NE regional composite seismic sections, spanning from deep offshore to onshore (location in Figure 1), illustrate the structural configuration of the Niger Delta (Figure 11). These depth-converted sections reveal the progressive transition from updip extension to downslope contraction, characteristic of gravitational collapse in the delta. The depth of the Oceanic Moho in the cross sections is derived from the integration of interpreted seismic data and previous work (e.g., Briggs et al., 2006, 2009, and references therein).

7.1. General Configuration of the Delta System

The cross sections of Figure 11 show the four main tectonic provinces of the study area: (a) an updip extensional domain onshore and across the continental shelf, (b) a domain characterized by strong shale mobility; (c) a translational domain along the mid-slope, and (d) a contractional domain in deepwater (Figure 11). These structurally linked regions are well-documented in salt- and other shale-bearing margins (e.g., Brun & Fort, 2018; Cramez & Jackson, 2000; Dooley et al., 2020; Fort et al., 2004; Haack et al., 2000; Oliveira et al., 2012; Rowan, 2020; Rowan et al., 2004).

The stratigraphic framework used in Figure 11 follows the chronostratigraphic scheme in Figure 2 and is regionally calibrated by wells. We introduce two updates. First, we identify the tops of the Lower Miocene and

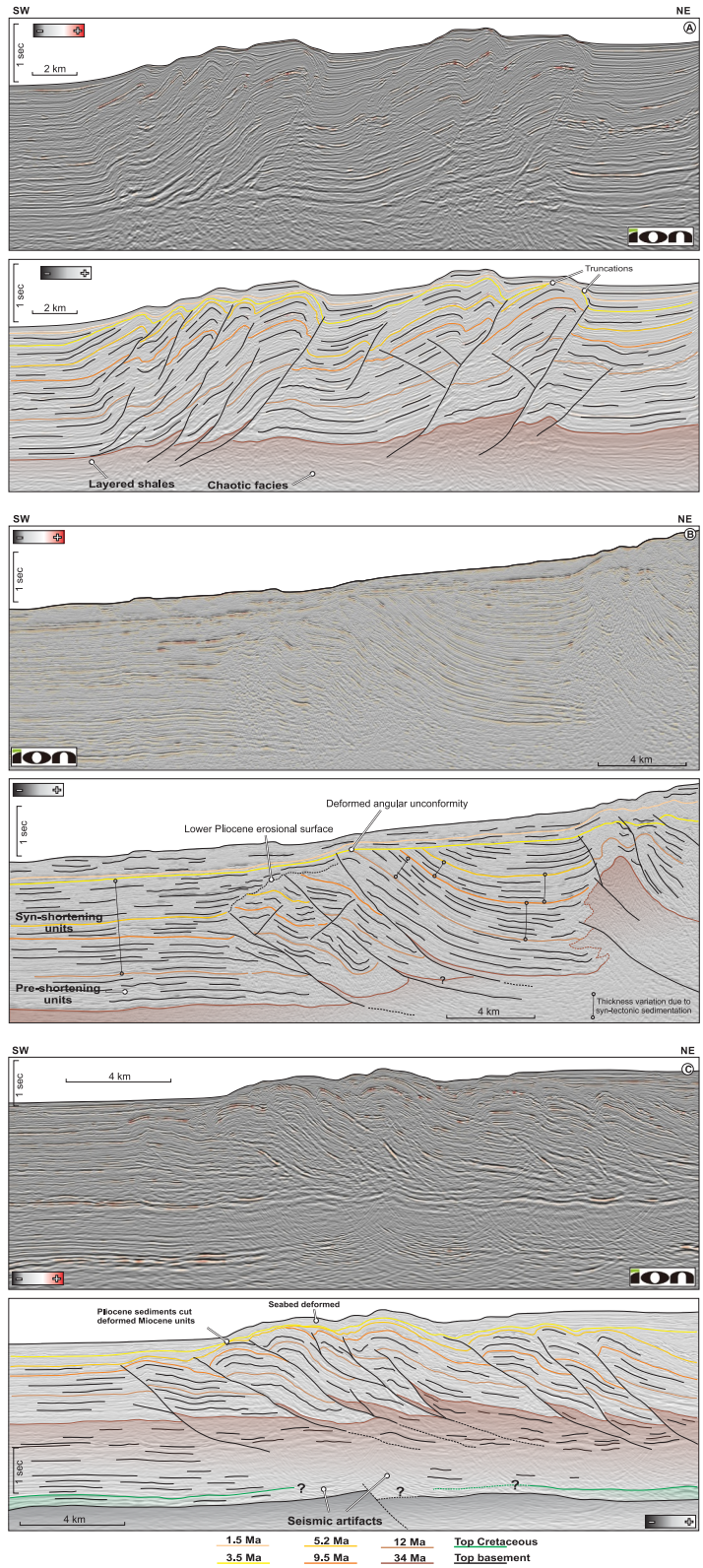

Figure 10. Seismic examples and interpretation of mobile shales in the deepwater fold–thrust belt. (a) Back-thrusting, (b) seaward thrusting, and (c) seaward thrusting involving mobile shales, which are internally deformed by multiple detachments and show evidence of some internal flow. See location in Figure 3. The pseudo-relief filter applied to the seismic lines enhances contrast and emphasizes the continuity of seismic reflections. Uninterpreted, higher-resolution versions of (a), (b), and (c) are provided in Figures S3–S5 in Supporting Information S1, respectively.

10.1029/2024TC008689

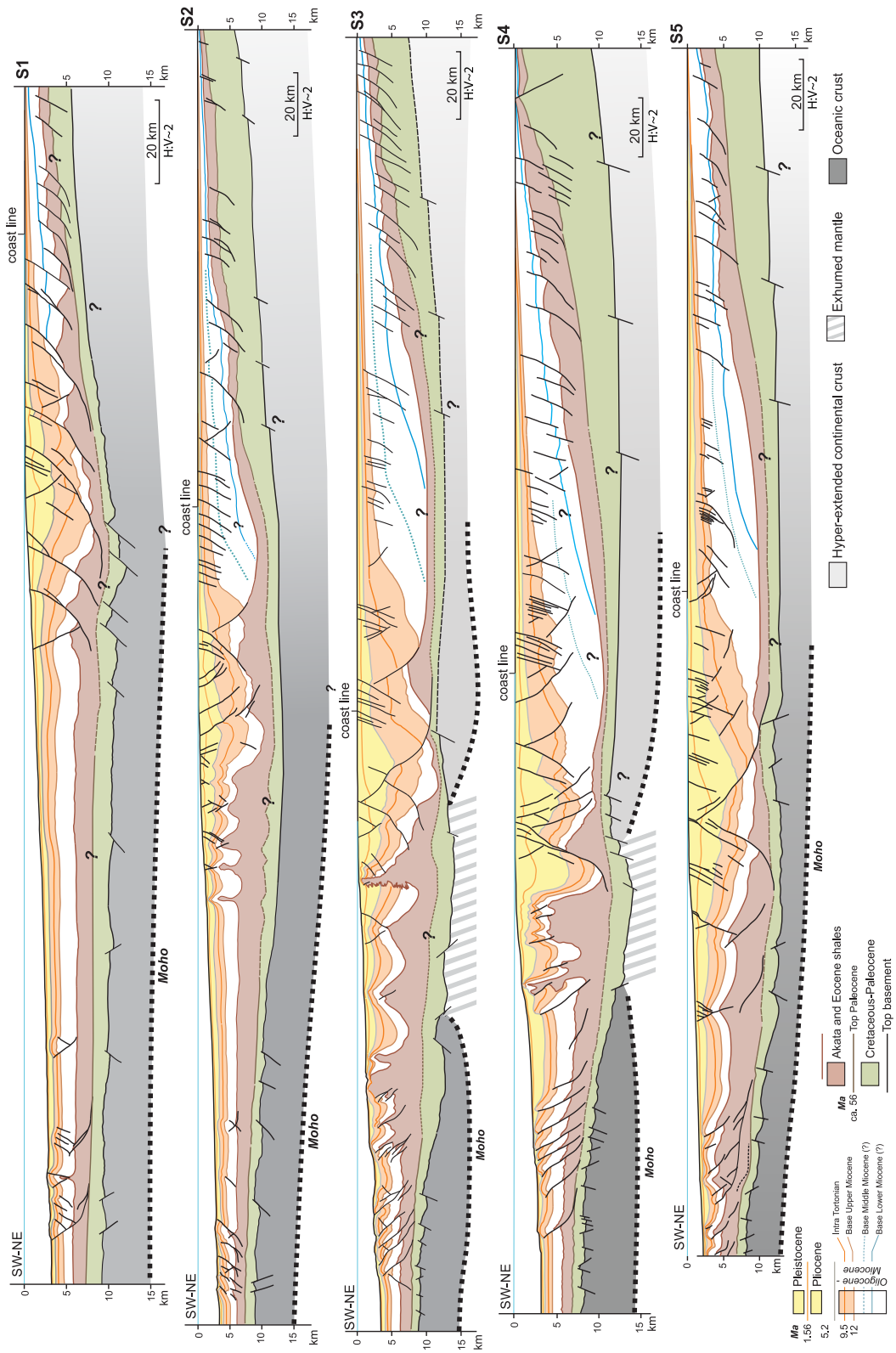

Figure 11. Five regional cross sections in depth of the Niger Delta system (S1 to S5; location in Figure 1a), each with its own vertical exaggeration (not at 1:1 scale). The location of these sections is also marked in the higher-resolution bathymetry map provided in Supplementary Figure S6.

Paleocene series. Second, within the Eocene and Akata age successions, we distinguish between mobile and relatively immobile shales, recognizing that this transition is gradual.

In all sections, the extensional domain extends from the onshore region to the continental shelf, where listric normal faults detach within the thin Akata shales (Figure 11). Although the basal sequence is not fully imaged, previous studies suggest that the Akata shales overlie a basinward-dipping basement covered by a thin Cretaceous–Paleocene sequence (e.g., Adegoke et al., 2017; Doust & Omatsola, 1990; Ekweozor & Daukoru, 1994; Evamy et al., 1978; Obaja, 2009; Stacher, 1995; Whiteman, 1982). The age of normal faulting decreases basinward, as indicated by syn-tectonic Miocene sequences (e.g., Sections S2 and S4 in Figure 11).

Extensional faults in the shallow offshore exhibit listric geometries, detaching in the lower Akata shales at ∼10 km depth and forming hanging-wall growth strata (Sections S1, S4, and S5 in Figure 11). In the central and eastern sections, normal faults shift from basinward-dipping to landward-dipping (counterregional) near the coast (Sections S3, S4, and S5 in Figure 11) (e.g., Ajakaiye & Bally, 2002; Cohen & McClay, 1996; Damuth, 1994; Haack et al., 2000). This polarity shift likely occurs over a domain with exhumed mantle, marking the transition from oceanic to continental lithosphere. Similar polarity reversals have been documented in other shale-dominated margins (e.g., Espurt et al., 2009; McClay et al., 1998, 2003; Morley & Guerin, 1996). The most distal landward-dipping fault defines the boundary with the translational domain, which is characterized by high-relief shale ridges (Figure 11).

Maximum accumulations of mobile shales occur in the central delta (Sections S1–S5 in Figure 11), reaching thicknesses of 5–7 km (e.g., Section S4). Mobile shales form high walls and broad anticlines that developed from Miocene to the present, becoming increasingly asymmetric basinward. As they advance, they evolve into outward-verging thrusts, with some landward-thickening wedges (e.g., Sections S3 and S4 in Figure 11).

The transition to the contractional domain is gradual in all sections, occurring near the basement hinge, where the slope flattens to a subhorizontal morphology. This observation agrees with the geometries documented in experimental models of salt systems (e.g., Dooley et al., 2007). In the Niger Delta the transition to the contractional domain is marked by thinning Akata shales, decreasing thrust dips, and reduced spacing between fault-related folds (Figure 11). In the western sections (S1 and S2) this transition is less pronounced, as the Akata shales and overlying strata remain sub-horizontal and largely undeformed, except for isolated pop-up structures.

The deepwater contractional domain consists of shale-involved thrusts and associated fault-propagation folds, occasionally forming "fishtail" thrusts (e.g., Sections S1 and S3 in Figure 11). These thrust faults, active since the Miocene, become progressively younger basinward (Krueger & Grant, 2011; Leduc et al., 2012). They detach within the upper Akata shales (Briggs et al., 2006; Cobbold et al., 2009; Corredor et al., 2005; Leduc et al., 2012; Morgan, 2003) along intra-shale horizons (Figure 10; Sections S1, S3, and S4 in Figure 11). Shortening involves both the Upper Akata Formation and part of the Eocene shales (Lower Akata Formation). Contraction varies in style from brittle thrusting and shearing along discrete surfaces to distributed ductile flow and disharmonic folding inflating fold cores [similar to Bilotti and Shaw (2005), Maloney et al. (2010), and Zhang et al. (2021)]. The FTB is generally directed oceanward, except in section S2, where it is directed landward (Figures 10a and 11). Lateral changes in thrusting direction are common in shale-involved folds (e.g., Butler et al., 2019; Higgins et al., 2009; Soto & Hudec, 2023; Wu et al., 2020).

The delta front is identified in sections S1, S3, and S4 by a gently dipping thrust, typically buried (Figure 11) [see also Maloney et al. (2010) and Jolly et al. (2016)]. Notably, mobile shales do not emerge in deepwater, preventing an open-toe system as observed in some salt margins (e.g., Dooley et al., 2022; Granado et al., 2023; Hudec & Jackson, 2007).

7.2. Strain Distribution in the Delta

Two cross sections, across the western (S1) and eastern (S5) lobes (Figure 11), were restored to estimate bulk strain across the basin (Figure 1). This restoration does not account for internal shale deformation, volume changes, or basement faulting (see data set and methods). Another key simplification is that we have treated all sequences from the Akata Formation to the basement top as a single shale unit. Table 1 summarizes the extensional strain in the updip domain and the amount of shortening along the outer fold belt.

Table 1
Comparison Between the Extension in the Updip Domain and the Shortening at the Toe of the Gravitational System, Based on Regional Cross Section S1 and S5 (Figure 11)

Geological cross section	Structural domain	Length (km)	Updip extension km	Updip extension %	Downdip shortening km	Downdip shortening %
Regional cross section S1 (Figures 11 and 12)	Western lobe	307	22	14	3	4.0
Regional cross section S5 (Figures 11 and 13)	Eastern lobe	370	18	6	4	4.5

The sequential restoration of section S1 (Figure 12) indicates that extension has consistently exceeded shortening along the gravitational system's toe. The comparison between the present-day configuration of section S1 (Figure 12a) and the restoration of the 12 Ma surface (near the base Tortonian, Upper Miocene series; Figure 12e) suggests a global net extension of approximately 19 km (5%) resulting from an estimated updip extension of ∼22 km (14%) and ∼3 km (4%) of shortening (Table 1). The top of the Eocene shales was already structured offshore by gentle highs and lows, while onshore it was affected by basinward-dipping normal faults (Figure 12e). Since the Pliocene (Figures 12c and 12d), the reduction in shale thickness in the onshore area decreased their

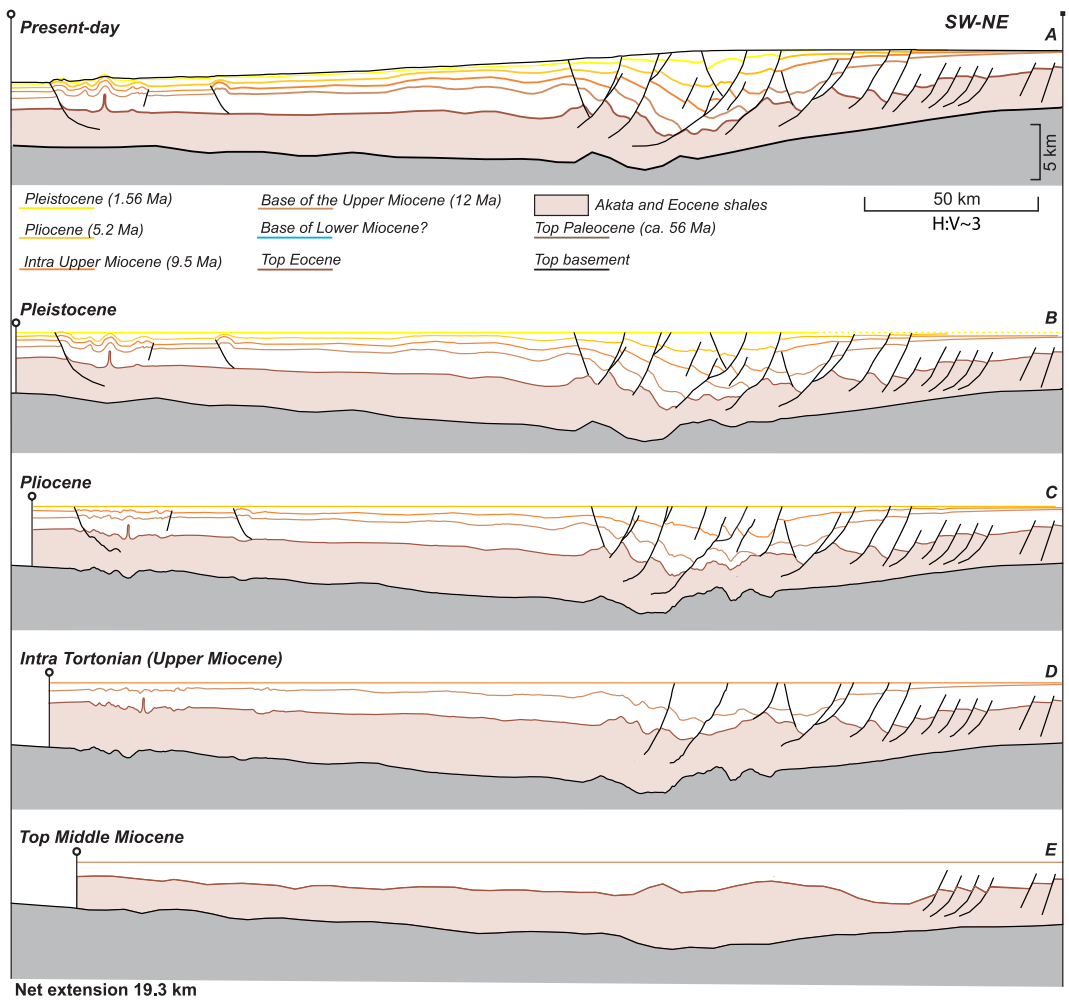

Figure 12. Sequential restoration (steps a–e) of cross section S1 up to the top of Middle Miocene stage at 12 Ma (see Figure 1a for location). Restoration documents an overall extension of the section of about 19 km (Table 1). All panels are drawn with the same vertical exaggeration (not at 1:1 scale), as indicated in the figure. The gray infill shows the sequences beneath the Akata Formation and the Eocene shales without distinction, including the basement.

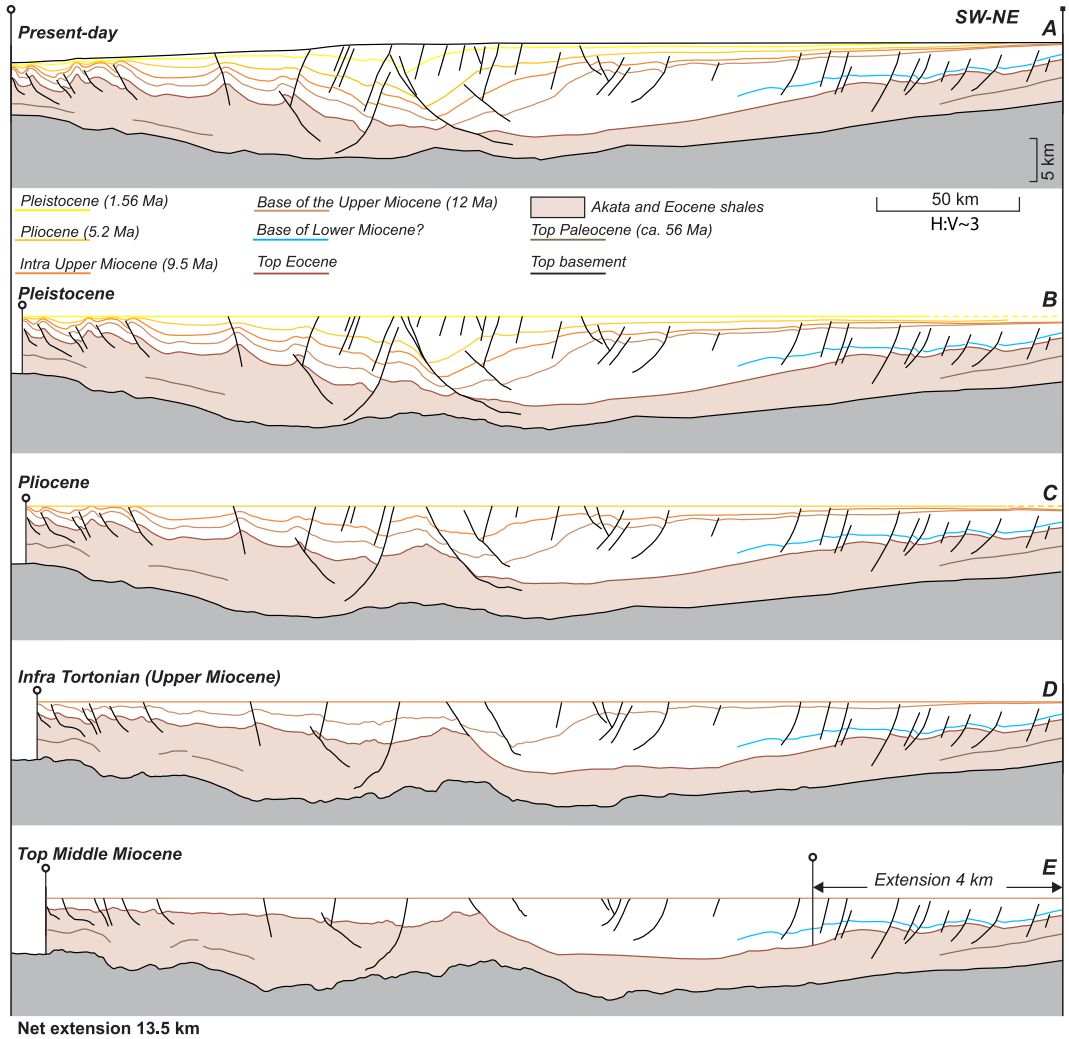

Figure 13. Sequential restoration (steps a–e) of cross section S5 up to the top of Middle Miocene stage at 12 Ma (see Figure 1A for location). Restoration documents an overall extension of the section of about 14 km of the Cenozoic section (Table 1). An earlier Cenozoic extensional deformation is documented by faulting (4 km of extension) in the internal domain of the delta (Table 1). All panels are drawn with the same vertical exaggeration (not at 1:1 scale), as indicated in the figure. The gray infill shows the sequences beneath the Akata Formation and the Eocene shales without distinction, including the basement.

ability to flow, promoting differential subsidence and stress redistribution, which contributed to the formation of south-dipping listric faults.

The restoration of section S5 shows progressive downslope shale inflation driven by differential subsidence exerted by the Miocene–Pleistocene supra-shale wedges (Figure 13). Since the Late Miocene, both landward- and basinward-dipping normal faults developed in the upper portion of the mobile shales (Figures 13a to 12d). The comparison between the present-day configuration of section S5 (Figure 13a) and the restoration of the 12 Ma surface (near base of the Tortonian, Upper Miocene series; Figure 13e) suggests a global extension of about 13 km (4%). In particular, the 12 Ma restoration suggests a total ~18 km (6%) extension and ~5 km (4.5%) shortening (Table 1). The estimated amount of shortening (Table 1) must be considered as a minimum, since this cross section does not comprise the entire outer FTB (Figure 1a).

The integration of the shortening estimated by Pizzi et al. (2020) along two cross sections parallel to the S5 and encompassing the entire outer FTB highlights an important difference between updip extension and downdip shortening. Our results, which do not vary significantly, are consistent with such estimates. Pre-Tortonian updip

extension is estimated as amounting to ∼4 km (5%) (Figure 13e). It is important to notice the progressive development of a major landward-dipping fault in the central portion of the section, which coincides with an important trough in the basement (e.g., since Figure 13d).

Regionally, the width of the deepwater FTB and its shortening vary laterally, reflecting differences in deformation intensity and strain partitioning across the margin (e.g., Bilotti & Shaw, 2005; Corredor et al., 2005; Krueger & Grant, 2011). In the northern sector, shortening since the Late Miocene is ∼6% (∼6 km), increasing to ∼13% (∼10 km) in the western lobe's central part and ∼15% (∼14 km) in the eastern lobe. These values align with previous estimates (Pizzi et al., 2020). The previously mentioned imbalance between updip extension and downdip shortening has been explained by invoking various processes (e.g., Krueger & Grant, 2011; Pizzi et al., 2020; Restrepo-Pace, 2020; Suppe, 2011). These include: (a) the existence of complex (sub-seismic) structures associated with faults and folds, (b) far-field flow of the weak shales, (c) distributed shearing within and at the top of the Akata shales, and/or (d) lateral compaction of these weak units, leading to increased pore pressure and associated fluid-escape.

8. Architecture of the Delta

This section examines the large-scale stratigraphic and structural architecture of the offshore domain of the Niger Delta, using time maps constructed for key Miocene to Quaternary geological horizons (Figure 14 and Figures S7–S12 in Supporting Information S1). The lack of well calibration and the generally poor quality of seismic data in deeper units hinder the construction of reliable regional seismic maps for the Cretaceous to Eocene units. To address this, we integrate seismic maps (Figures 14–16) with isochore maps (Figure 15) to highlight the spatial and temporal distribution of Cenozoic depocenters. These interpretations provide constraints on the timing of deformation across the Niger Delta. Additionally, long-offset regional seismic lines (Figure 17) help outline the basin's overall geometry and discuss the influence of crustal structures on shale tectonics.

8.1. Structural Configuration of the Supra-Shale Section (the Agbada Formation)

Time structural maps highlight structural geometries at different stratigraphic levels within the Agbada Formation, that is, the supra-Akata section. We focus on the intra-Lower Pleistocene level (1.56 Ma), which is shown in Figure 14a. Additional structural maps for older intervals—3.5 Ma (intra-Upper Pliocene), 5.2 Ma (lowermost Lower Pliocene), 9.5 Ma (intra-Tortonian, Upper Miocene), and 12 Ma (near the base of the Tortonian)—are provided in the (Figures S7–S19 in Supporting Information S1). The base of the post-Akata Formation succession is illustrated in Figure 14b.

The structural map for the intra-Lower Pleistocene reflector reveals a shallow, almost flat sector along the continental slope, interrupted by a large structural through approximately 50 km wide and parallel to the coastline (Figure 14a). This trough is associated with both landward- and basinward-dipping normal faults, which rarely exceed 30 km in length. Isochore maps of the intervals between 1.56 and 3.5 Ma (Figure 15a) and between 3.5 and 5.2 Ma (Figure 15b) indicate that these depressions correspond to thick fault-controlled depocenters. In these areas, the thickness of the sediments exceeds 1 s TWT (Figure 15a) and 3.5 s TWT (Figure 15b). This suggests active sedimentation during normal faulting.

Moving basinward into the “diapir” domain of the western lobe and the Triangular Bulge (Figure 3), all discontinuities exhibit deformation across the entire stratigraphic record (Figures S7–S11 in Supporting Information S1). This results in wide, rounded highs and narrow lows or troughs. A comparison between isochore and time maps suggests that these lows correspond to thick depocenters, while structural highs consist of thin and condensed stratigraphic sequences (Figures 15a–15e). Notably, these structures have not been observed in the eastern lobe.

Narrow structural highs, oriented NNW–SSE to NW–SE, with maximum lengths of approximately 40 km, are also observed within the inner FTB of the western lobe (Figure 14). This sector narrows progressively toward the Charcot fracture zone, becoming nearly indistinguishable in the eastern lobe.

In the transition zone, which encompasses both the western and eastern lobes, the intra-Lower Pleistocene (1.56 Ma) and intra-Upper Pliocene (3.5 Ma) surfaces remain nearly undeformed (e.g., see Figure 14a) and are regionally relatively thin (Figures 15a and 15b). Isochore maps indicate that the Pliocene–Pleistocene sediments (between 1.56 and 3.5 Ma) have a maximum thickness of ∼0.2 s TWT (Figure 15a). In contrast, the Lower to

10.1029/2024TC008689

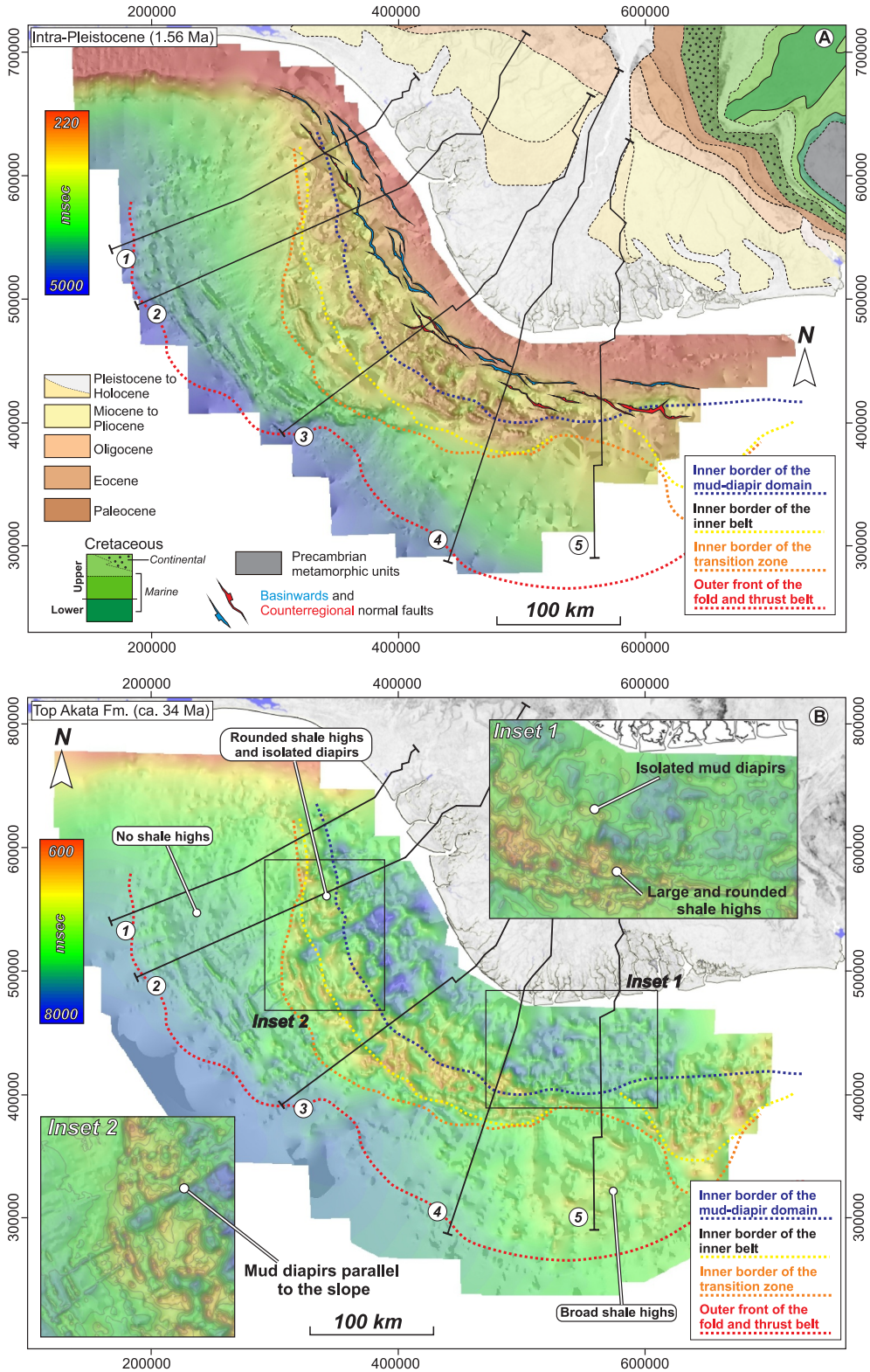

Figure 14. (a) Time map of the intra–Pleistocene stratigraphic level (1.56 Ma) in the offshore domain of the Niger Delta. (b) Time map of the top Akata Formation (top Eocene, at ~34 Ma). Inset 1 (upper right) details the geometry of isolated diapirs in the marginal domain of the delta. Inset 2 (lower left) illustrates the geometry of mobile-shale walls aligned parallel to the slope in the intermediate domain of the delta. Larger version of these maps is provided in Figures S8 and S12 in Supporting Information S1, respectively.

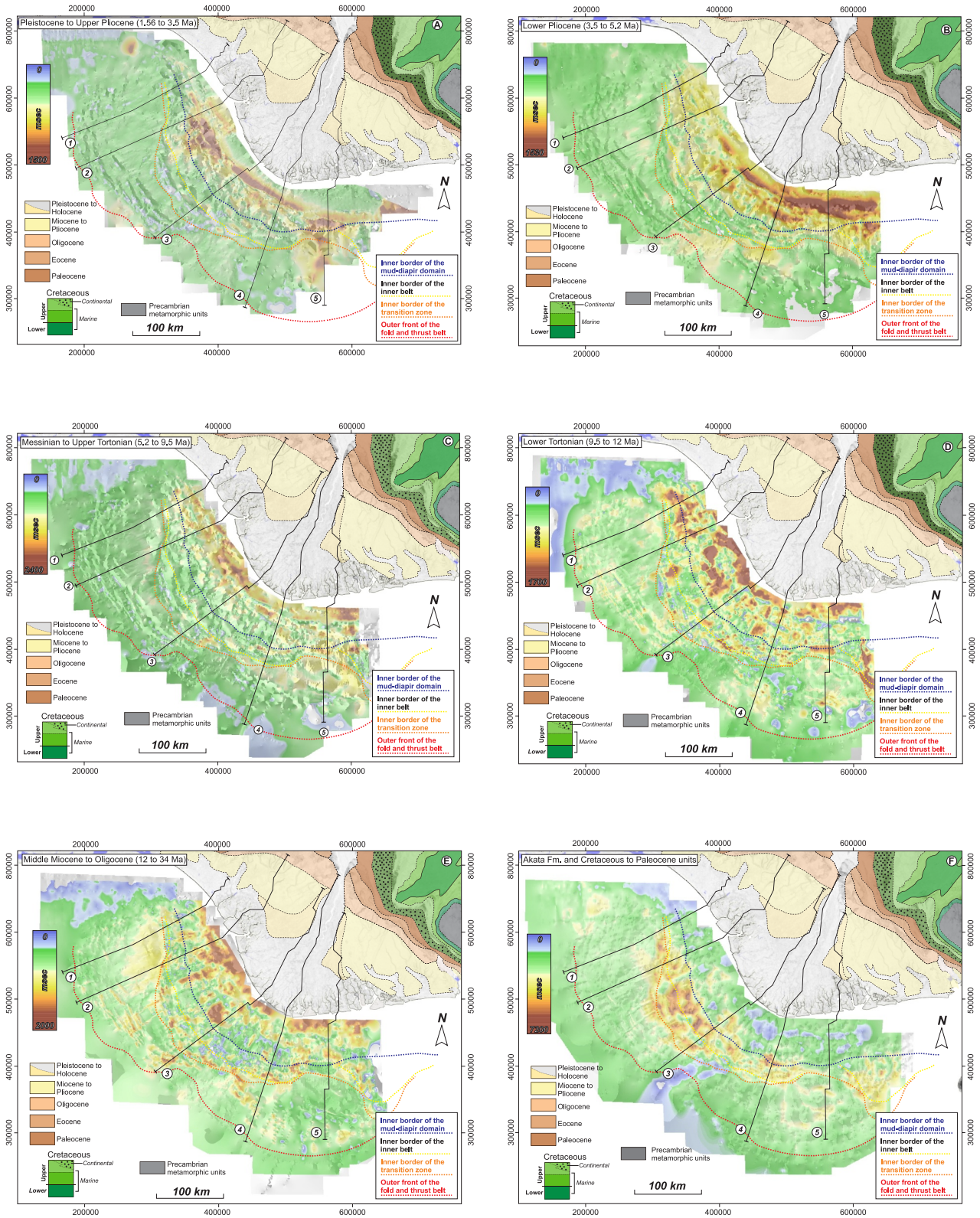

Figure 15. Isochore maps of the different stratigraphic units of the delta (see Figure 2): (a) 1.56 to 3.5 Ma (Pleistocene to Upper Pliocene), (b) 3.5 to 5.2 Ma (Lower Pliocene), (c) 5.2 to 9.5 Ma (Messinian to Upper Tortonian), (d) 9.5 to 12 Ma (Lower Tortonian), (e) 12 to 34 Ma (Middle Miocene to Oligocene), and (f) the sequences between top basement and top Akata Formation. Dashed lines mark the boundaries of the structural domains identified by Corredor et al. (2005), mapped at the seabed (Figure 3). Uninterpreted, higher-resolution versions of these maps including countours are provided in Figures S13–S18 in Supporting Information S1.

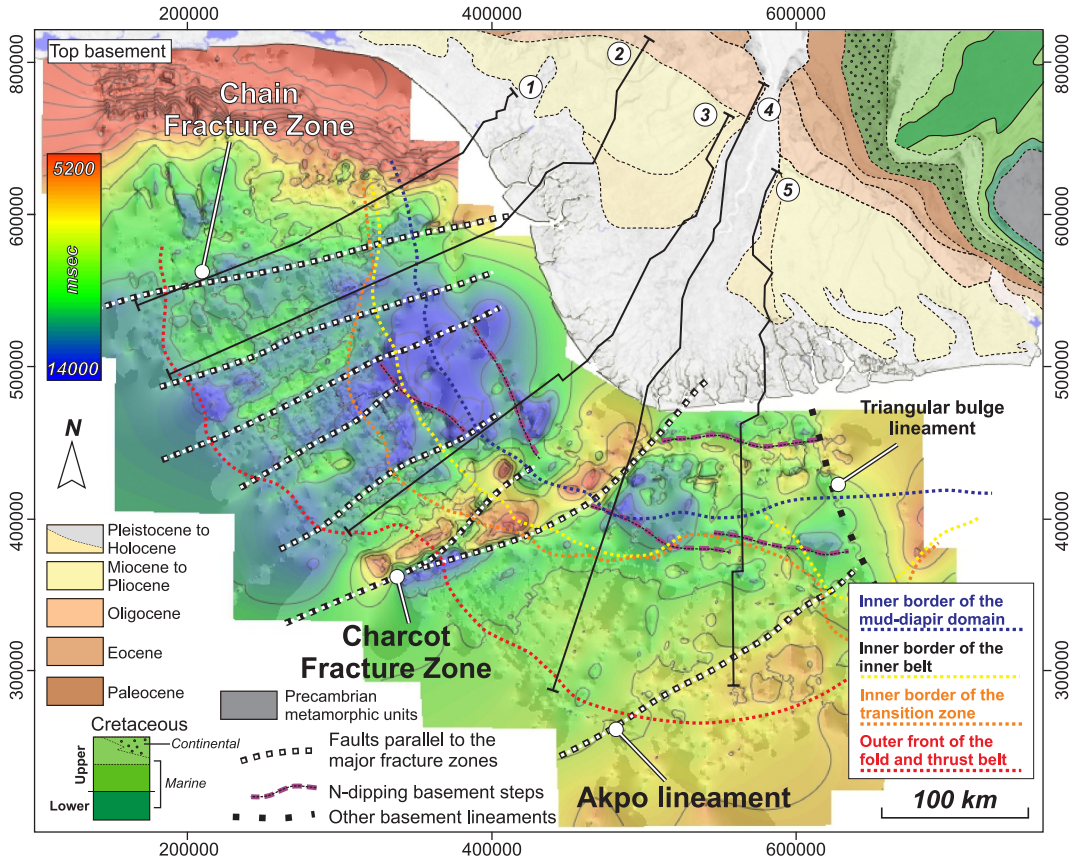

Figure 16. Time contour map (contour interval 0.5 s TWT) of the top basement including the main faults affecting this surface, such as longitudinal (SW–NE) oceanic fracture zones and transverse (north-dipping or "counterregional") faults. An uninterpreted, higher-resolution version of this map is provided in Figure S19 in Supporting Information S1.

Upper Pliocene sediments (between 3.5 and 5.2 Ma) exhibit thicknesses varying between ~0.4 and 0.7 s TWT (Figure 15b).

In the eastern lobe, particularly near regional Section 5 (Figures S7–S19 in Supporting Information S1), intense deformation affects the Miocene to intra-Upper Pliocene sequences. Folds, often thrust-related and thrust-propagation structures, are oriented WNW–ESE and NE–SW (Figure 9). As previously mentioned, these structures deform an almost isopachous seismic package of Upper Miocene age and are interpreted to have formed between 9.5 and 5.2 Ma (cf. Figure 8). The rate of fold growth progressively decreases during the Upper Pliocene, as indicated by the flat and undeformed surfaces of the 1.56 and 3.5 Ma discontinuities (Figures 14, 15a, and 15b).

At the toe of the Niger Delta, throughout the external FTB, both structural and isochore maps reveal continuous deformation across all stratigraphic surfaces (Figure 14a and Figures S7–S10 in Supporting Information S1), extending to the seabed (Figures 3 and 10). In this domain, tectonic structures are characterized by narrow, NW–SE trending thrust-related anticlines in the western lobe and WNW–ESE trending ones in the eastern lobe. Near the termination of the western lobe, the lateral continuity of these structural trends is distinctly interrupted around the Charcot fracture zone (Figures 14 and 15).

8.2. Geometry of the Akata Shales

The time map for the top Akata shales (i.e., top Eocene; Figure 14b) reveals structures consistent with those observed within the Agbada Formation at different stratigraphic levels (Figures 14a and 15a–15e). However, the

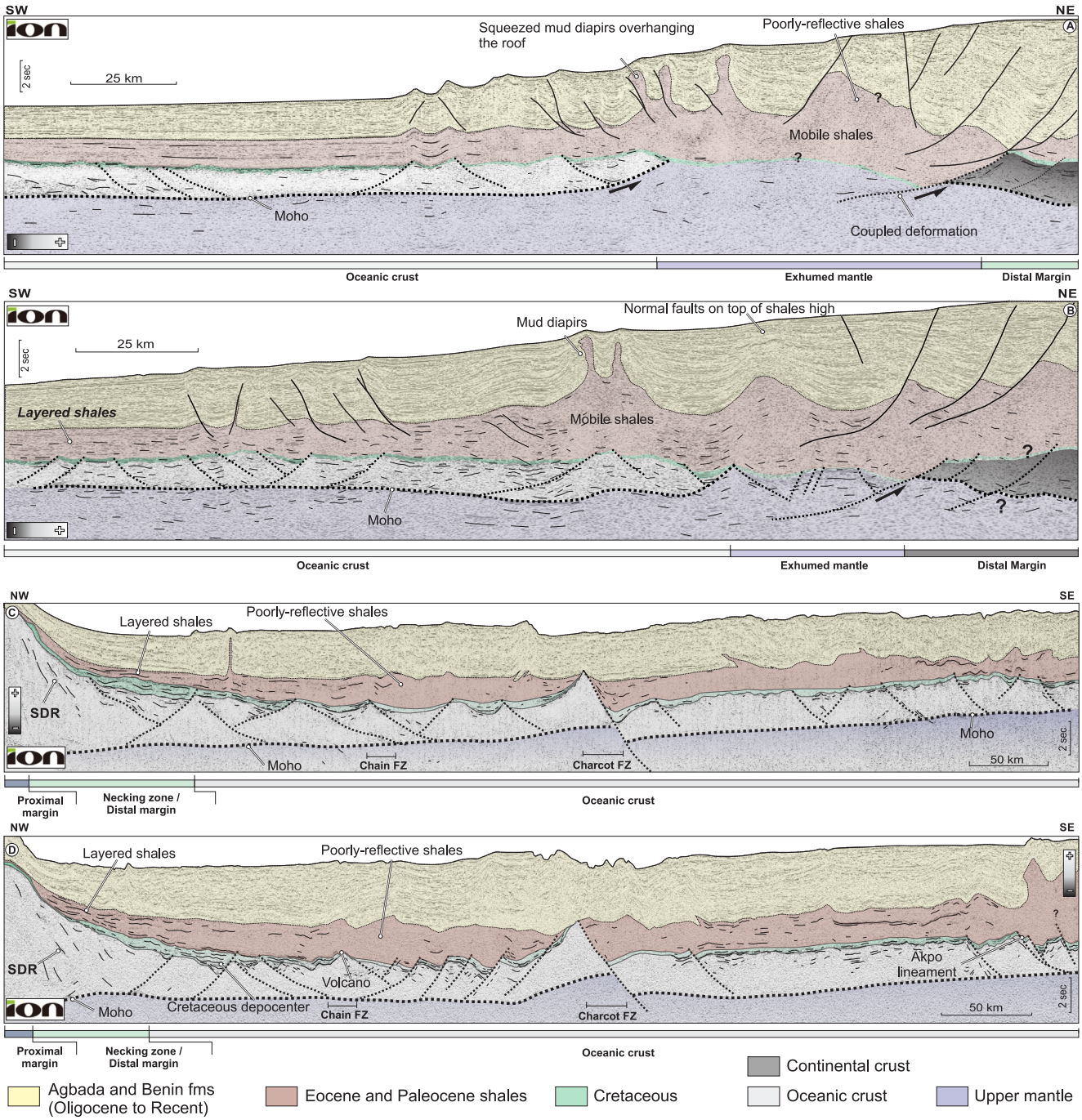

Figure 17. Long offset crustal seismic lines showing the general structure of the delta system and the crustal architecture of the margin (see Figure 3 for location). (a) and (b) Transverse dip lines across the margin in the western lobe of the delta. (c) Composite line running along the distal domain of the delta. (d) Seismic composite line extending across the intermediate domain of the delta. Moho discontinuity and fracture zones are also indicated. Uninterpreted, higher-resolution version of these seismic lines are provided in Figures S20 and S21 in Supporting Information S1.

Akata Formation as a whole (Figure 15f) exhibits additional structures that are not apparent on its upper surface (Figure 14b).

The shallow offshore sector, which is part of the extensional domain, is characterized by a broad area (~50 km wide) of thin shales (~0.3 s TWT) at depths exceeding 7 s TWT (Figures 14b and 15f). These thin shales at great depths extend parallel to the present-day coastline and shapes isolated NW–SE to WNW–ESE highs, along with

diapiric structures (Inset 1 in Figure 14b). Southward, this sector transitions into a region roughly corresponding to the "diapir" domain and the inner belt, where the shales are highly deformed (Figures 14 and 15f). This region is characterized by broad NW–SE shale highs, aligned with the basin slope and exhibiting rounded external shapes (Figure 14b). In the western lobe, two NE–SW structural lows disrupt their lateral continuity.

Across the Charcot fracture zone, the width of the "diapir" domain and the inner belt zone decreases significantly, from ~87 km in the western lobe to ~40 km in the eastern lobe (Figures 14b and 15f). Similar mobile-shale highs are observed further east in the Triangular Bulge (Figure 15f). In the transition zone within the western lobe, the Akata shales remain relatively undeformed, whereas large WNW–ESE and NE–SW culminations dominate the eastern lobe (Figures 8, 14b, 15f). At the toe of the gravitational system, within the external FTB, the Akata shales are deformed by NW–SE thrust-related anticlines (Figures 10a, 10c, and 14b).

8.3. Basement Configuration

The top basement time map, as illustrated in Figure 16, exhibits significant structural variability, with elevations ranging from deep subsiding regions to prominent elongated structural highs. These variations define the main structural framework of the area. The dominant feature is a series of individual elongated highs, associated with the Charcot Fracture Zone (FZ). This major SW–NE-trending high extends from deepwater to near the shoreline, dividing the delta into two general domains: the western and eastern delta.

These ridges and depressions are particularly evident in the western delta (Figure 16). On the contrary, the eastern domain, up to the Triangular Bulge high in the extreme east, is characterized by a gently south-dipping basement with a local, wide deep trough in the north (>11 s TWTT). In general, uplifted basement blocks create distinct high-relief areas that influence the overlying stratigraphic infill (cf. Figure 15). In contrast, lower-relief regions correspond to subsiding zones that have accommodated thick accumulations of sediments, including the Akata shales, as illustrated in Figure 15f. This relationship underscores the role of basement geometry in controlling sedimentation patterns and deformation in the region.

This structural complexity is further influenced by a network of major fractures and structural lineaments that affect the basement geometry (Figure 16). Examples of these faults include the Chain FZ and the Akpo Lineament, both trending SW–NE.

These faults, along with numerous unnamed fractures, extend across the entire basement surface, from deepwater areas to the shallow platform domain. Their orientation and distribution appear to control the overlying Akata shales and the lowermost sequence of the Agbada Formation (Oligocene–Middle Miocene), as their influence is visible in both sequences (Figures 14b and 15e). In the younger sequences of the Agbada Formation (Lower Tortonian to Recent), the influence of these faults on the stratigraphic architecture is less evident. They mainly generate a series of gentle highs and lows, oriented perpendicular to the seafloor slope and coinciding with the boundaries between the different tectonic domains of the delta (Figures 15a–15d).

The basement morphology strongly influences the distribution and deformation of mobile shales (e.g., Morgan, 2003; Spina & Mazzoli, 2023). Basement highs are closely associated with the inner FTB, while the transition zone and the outer FTB align with deeper basement areas, promoting detachment and deformation of the overlying sediments (Figures 15f and 16). Additionally, basement depressions coincide with the inner border of the "diapir" domain, suggesting a link between fault-controlled basement subsidence and shale mobilization.

8.4. Crustal Structure

The horizontal derivative of the Bouguer anomaly highlights gravity variations, mostly reflecting crustal structures and density contrasts (Figure 18a). High-gradient areas (red and blue) indicate abrupt changes in basement configuration, with major fault corridors (e.g., Chain FZ and Charcot FZ) marking structural discontinuities.

NE–SW anomalies onshore likely correspond to basement horsts and grabens bounded by normal faults, shaping the Anambra and Bida basins as well as the Benue Trough (Figure 18b). The main structural trends observed in the shallow offshore area, including the extensional domain and the "diapir" zone, are also evident in the Bouguer map (Figure 18b). An important positive anomaly parallel to the shoreline is observed in the shallower platform area. This elongated feature, located in the central region of the delta, likely corresponds to the thick Agbada depocenter observed in Sections 3 and 4 (Figure 11), suggesting deep evacuation of the mobile Akata shales.

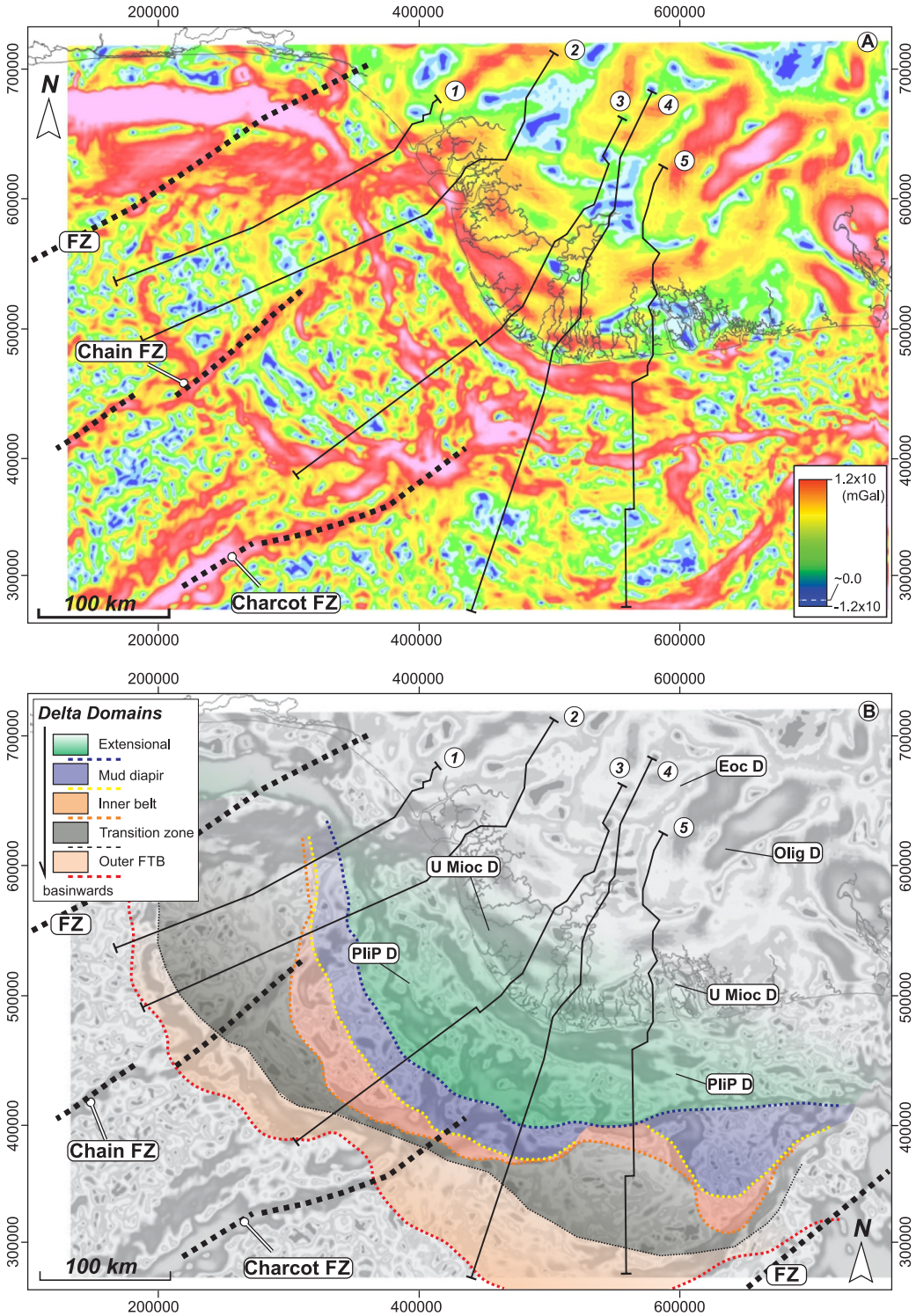

Figure 18. (a) Horizontal derivative of the Bouguer anomaly of the Niger Delta. The main fracture zones affecting the offshore domain of the Niger Delta are clearly identified, whereas positive anomalies onshore correspond to deep basement troughs. (b) Structural domains of the delta (from Figure 3) overlain on the horizontal derivative of the Bouguer anomaly (from a). Abbreviations: Chain FZ, Chain Fracture Zone; Charcot FZ, Charcot Fracture Zone; EocD, Eocene depocenter; FZ, Fracture zone; Olig D, Oligocene depocenter; PliP D, Pliocene–Pleistocene depocenter; UMioc D, Upper Miocene depocenter. Larger version of the Bouguer anomaly maps in Supplementary Figure S22.

Further basinward, gravity anomalies define the structural segmentation of the delta. The inner FTB, the transition zone, and the outer FTB correspond to a series of alternating positive and negative anomalies (Figure 18b). These anomalies reflect lateral variations in gravity load, controlled by alternating elongated anticline culminations and syncline troughs within the mobile substrate.

The overall crustal and basin configuration of the margin is illustrated using two dip-oriented and two strike-oriented deep seismic lines, which run subperpendicular to the slope (Figure 17). The sedimentary infill is subdivided into three units: (a) the Agbada Formation (Oligocene–Recent), (b) the mobile shale unit, which comprises the Eocene Akata shales and Paleocene series, and (c) the deepest sequences, interpreted as Upper Cretaceous. We also differentiated the oceanic and continental crusts in these sections, and the position of the reflective package marking the Moho.

Three key features are observed along the dip lines: (a) A highly stretched domain of the continental crust in the lower continental slope, coinciding with the thickest accumulation of mobile substrate (Figures 17a and 17b). (b) As a consequence, broad "diapiric" anticlines and the transition to basinward faulting and downslope shale gliding occur above this highly stretched crust. In some cases, mobile shales directly overlie exhumed mantle (Figure 17b). (c) The Cretaceous series occur discontinuously along the margin, reaching maximum thickness in basement half-grabens (Figures 17c and 17d).

These half-grabens are probably oblique to the main trends of the tectonic domains of the delta, as they are more evident in the sections running perpendicular to basin slope (Figures 17c and 17d). The tilted blocks of the oceanic and highly stretched continental crusts are bounded by extensional faults detaching along the Moho.

In the oceanic domain, the Charcot FZ forms a first-order structural high, offsetting the oceanic basement with a vertical displacement exceeding 4.5 km (Figures 17c and 17d). The Agbada Formation directly overlies oceanic horsts in this area. As a consequence, the Charcot FZ separates two sub-basins with a contrasting configuration of the mobile substrate of the delta. These two delta lobes appear to have evolved independently and recorded different sedimentation rates since the Miocene (Chima et al., 2021 and references therein).

The overall margin geometry is characterized by a necking domain extending over 500 km onshore into the African continent. The seismic data also reveal an extreme thinning of the crust in the transition between continental and oceanic domains, characteristic of a hyperextended margin where the transition is marked by a domain of exhumed lithospheric mantle (Figures 17a and 17b). This transition ultimately leads to the Lower Cretaceous Atlantic oceanic crust (Heine et al., 2013; Figure 1).

These observations establish a structural framework to assess how basement configuration and crustal structure control the deformation of mobile shales, the development of the FTB, and the distribution of depocenters. The following discussion explores the implications of these findings for the tectonic evolution of the Niger Delta.

9. Discussion

In this section, we integrate our interpretations to address the scientific questions raised in the introduction: (a) What are the styles of mobile shales in the three structural domains of the delta (i.e., updip extension, "diapiric" region, and deepwater FTB)? and (b) How does the crustal architecture of the hyperextended margin control shale mobility within the delta system?

9.1. Structural Styles Associated With Shale Mobility

The offshore region of the Niger Delta is characterized by several contiguous depocenters filled with Miocene to Recent sediments, reaching thicknesses exceeding 6 s TWT (Figure 15). Chima et al. (2021) attributed stratal thinning toward shale-cored or thrust-related anticlines and thickening away from these structures (e.g., Figure 4) primarily to syn-depositional deformation, consistent with findings from other studies (Jolly et al., 2016; Krueger & Grant, 2011; Maloney et al., 2010; Morley et al., 2011). They suggested differential compaction as a possible alternative explanation, in line with observations from Maloney et al. (2010). However, the growth geometries in these minibasins, including sedimentary wedges and turtle-back structures (Figure 4c), indicate that thickness variations within these depocenters are inherently linked to shale mobility. In some instances, the supra-shale sequences (Miocene–Recent) are in direct contact with the basement, indicating the complete expulsion of the

underlying shales. This process results in the formation of primary welds (Figures 8c and 8d), analogous to those observed in salt systems.

Minibasin architecture suggests progressive subsidence and shale withdrawal, with shale flow feeding asymmetric mobile shale highs. We interpret that these highs started to grow since the Lower Miocene. This interpretation is supported by the occurrence of pre-kinematic sequences with constant thickness that are eventually upwarped due to the rise of mobile shale highs (e.g., Figures 4c and 8). However, this hypothesis requires further study and detailed analysis of higher-resolution 3D seismic data sets.

In the outer FTB, our observations in shale-cored folds align with recent descriptions by Spina and Mazzoli (2023). We also document the presence of detachment anticlines cored by mobile shales, deforming Upper Miocene–to–Recent growth strata (e.g., Figures 8b–8d). These folds progressively developed as their cores inflated. Shale inflation is accompanied by shale evacuation and withdrawal in the adjacent synclines, where progressive unconformities and wedges develop.

Basinward, shortening structures evolve into basin-directed listric thrusts and associated fault-related folds (Figures 9 and 10). These structures suggest the presence of duplexing through multiple detachments within the weak Akata shales. This deformation style involves significant internal decoupling levels within the shale sequences, rather than a single detachment at their base. Recent experimental models by Dooley et al. (2024) reproduce many of these structures, like duplexing and intra-shale detachments rooting supra thrust-related folds, further supporting this deformation style in mobile shales.

9.2. Significance of "Counterregional Normal Faults"

Basinward-thickening wedges of Miocene to Quaternary sediments, bounded by shales at their lower sections and faulted above, characterize the more distal part of the extensional domain of the delta (Figures 15a and 15b). The origin of these geometries has traditionally been attributed to the occurrence of landward-dipping faults (Chima et al., 2021; Corredor et al., 2005; Morley, 2003; Morley & Guerin, 1996). This type of faults is observed in many salt- and shale-margins (e.g., Rowan, 2020; Sapin et al., 2012; Van Rensbergen & Morley, 2003; Wu & Bally, 2000). Counterregional faults can result from tectonic extension, where the fault hanging walls move landward, that is, updip (Rowan et al., 2022; Rowan & Ratliff, 2012). Alternatively, they may originate from basinward expulsion of weak substrates (either mobile shales or salt), leading to expulsion rollovers (Diegel et al., 1995; Ge et al., 2019; Larberg, 1983; Schuster, 1995). This type of rollover requires large volumes of undercompacted shales at the base of major delta systems (Dailly, 1976). Some authors have also proposed that in the tectonic extension model, both footwall and hanging wall blocks move basinward, but the footwall moves faster and farther than the hanging wall (Brun & Fort, 2011; Brun & Mauduit, 2008).

Numerical models for shale margins show that shale mobilization occurs when fluid pressures approach lithostatic pressure (Albertz et al., 2009; Dean et al., 2015; Ings & Beaumont, 2010). One model by Ings and Beaumont (2010) represents a hyperextended margin with a crustal neck, where basinward shale flow occurs throughout the margin, promoting gliding and the formation of basinward wedges at the shelf break. These models reproduce several structures observed in the Niger Delta (Figure 10). However, they do not account for a key observation: the presence of multiple detachments within the weak basal shales in both extensional and compressional settings. This suggests that further modeling is needed to fully capture the complexity of shale deformation in the region.

Based on the structural style (Figure 11) and basin architecture (Figures 15a–15f), we propose that Miocene sediments prograded basinward over a thick, weak substrate of marine and pro-deltaic Paleocene–Eocene shales. The Miocene to Pleistocene evolution of the Niger Delta is schematized in different stages in Figure 19. The rapid progradation of delta wedges exerts a differential load on the underlying, less permeable shales, contributing to fluid retention. These processes are widely recognized in the region (e.g., Cobbold et al., 2009; Cohen & McClay, 1996; Morley & Guerin, 1996). We suggest that this configuration also led to local, total evacuation of the underlying shales. This implies two main outcomes: first, primary shale welding occurred where weak shales were entirely evacuated (e.g., Figure 8c); second, basinward-thickening wedges prograded into the accommodation space created by the general downslope flow and the local upbuilding of shales (e.g., Figure 8b). The final geometry resembles landward-dippingfaults limiting shale diapirs. However, we propose that they are better explained as expulsion rollovers, comparable to those formed in salt systems.

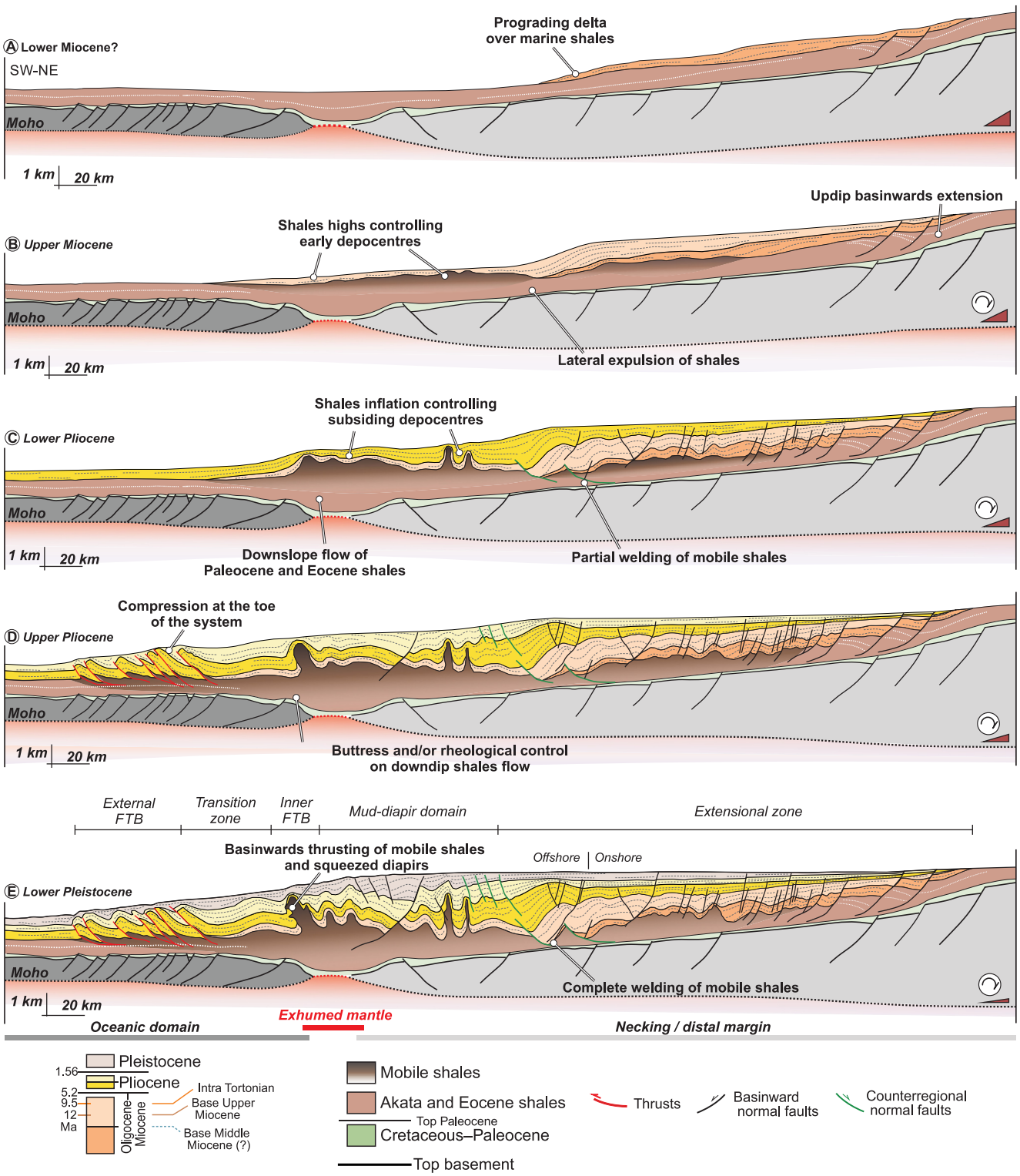

Figure 19. Schematic evolution of the Niger Delta illustrating the interplay between sedimentary progradation and the occurrence of mobile shales and associated structures. Red triangles and encircled arrows illustrate variations in the passive margin taper due to progressive tilting, respectively, resulting from the combined effects of margin subsidence/uplift and lithostatic loading caused by sediment accumulation in the delta.

9.3. Mobile Shales in the Hyperextended Margin

The interaction between delta progradation, gravity spreading, and shale flow in this segment of the West African passive margin is fundamentally controlled by its structural configuration and crustal architecture. The overall configuration of the margin and the delta system are illustrated in Figures 19 and 20, together with our interpretation of the distribution of the exhumed mantle domains and the variation in extension direction along the margin. The Niger Delta lies on a divergent margin segment of the west African passive margin and is characterized by a high degree of obliquity ($\alpha = 70°$) with respect to the active direction of extension. It is bounded laterally by two fault segments characterized by oblique extension and even transform margins (e.g., south of the Charcot FZ and north of the Chain FZ; Figure 20a). From deepwater to onshore, these fracture zones exhibit 15–20° variation in their orientation (Figures 16, 18a, and 20a). In other sectors of the Niger Delta located outside the study area, similar variations in the orientation of the faults affecting the top of oceanic crust have been observed. This change in strike could possibly indicate a change in the plate kinematics of the South Atlantic margins, which has not been captured by the model of Heine et al. (2013).

The processes operating in the Niger Delta margin are summarized in Figures 19 and 20. The overall structural configuration of the delta shows an updip extensional domain, transitioning into a deepwater region dominated by contraction, shale inflation, and mobile-shale walls. The various domains are linked by a region with large antiformal shale accumulations resulting from inflation, which encase deep minibasins.

Offshore, Paleocene–Eocene shales progressively thin out and are primarily characterized by distal facies and turbiditic sands. The accumulation of thick delta wedges, combined with post-rift thermal subsidence, led to the progressive tilting of the hyperextended crust of the passive margin. The structural response to this tilting includes the formation of listric faults in the updip delta, which accommodate extension and link to downslope contractional deformation in deepwater. Overpressure in the system originated from two key processes: (a) the rapid accumulation of Oligocene–Recent sediments over the shales, and (b) intense internal deformation within the weak shales, encompassing updip extension, downslope gliding, and downdip shortening.

The thickest accumulation of mobile shales coincides with a hinge in the basin slope, marking the transition from counterregional shale withdrawal in the extensional domain to shale upbuilding in the inner belt. This hinge also represents the onset of basinward contraction at the transition to the outer FTB (Figures 11 and 19). Additionally, this domain contains the exhumed mantle and is a crustal neck of the hyperextended crust (Figures 17, 19, and 20). The exhumed mantle coincides with the position of the deepest basement (Figure 16) and hosts the most substantial accumulation of mobile shales (Figure 15f). We propose that delta progradation progressively expels mobile shales, a process further amplified by the presence of the dense and less buoyant crustal neck at the ocean–continent boundary. This interpretation provides a geologically consistent framework compared to previous models, which depicted an undifferentiated, broad concave basement in this region (e.g., Albertz et al., 2009; Corredor et al., 2005; Wiener et al., 2010).

The sharp escarpment between the oceanic crust and the exhumed mantle is marked by a steep step (∼1 s TWT; Figures 17a and 17b). This basement escarpment roughly coincides with the basinward boundary of the region, marked by massive and tall mobile-shale walls (Figure 17). We propose that this escarpment may act as a local buttress, restricting the downslope flow of weak shales. In summary, mobile shales accumulated in this domain of the delta due to the combination of three factors: (a) a change in basin slope, which reduces the gravitational potential energy of the shales to downslope flow and gliding; (b) the local buttressing effect exerted by a basement step in the hyperextended margin, which is bounded by crustal faults; and (c) the presence of a denser neck consisting of exhumed mantle at the transition from the hyperextended crust to the oceanic crust.

Our analysis highlights the importance of shale mobility in shaping deltaic systems and their associated deformations. The structural evolution of the Niger Delta provides a compelling example of how shale tectonics can influence basin architecture. These findings underscore the need to refine numerical models to better account for multiple detachments, fluid overpressure, and the temporal evolution of shale mobilization. These considerations open new avenues for research on the broader implications of mobile shales in continental margins. Understanding the complex deformation patterns associated with mobile shales will be essential for refining predictive models and improving subsurface characterization in sedimentary basins worldwide.

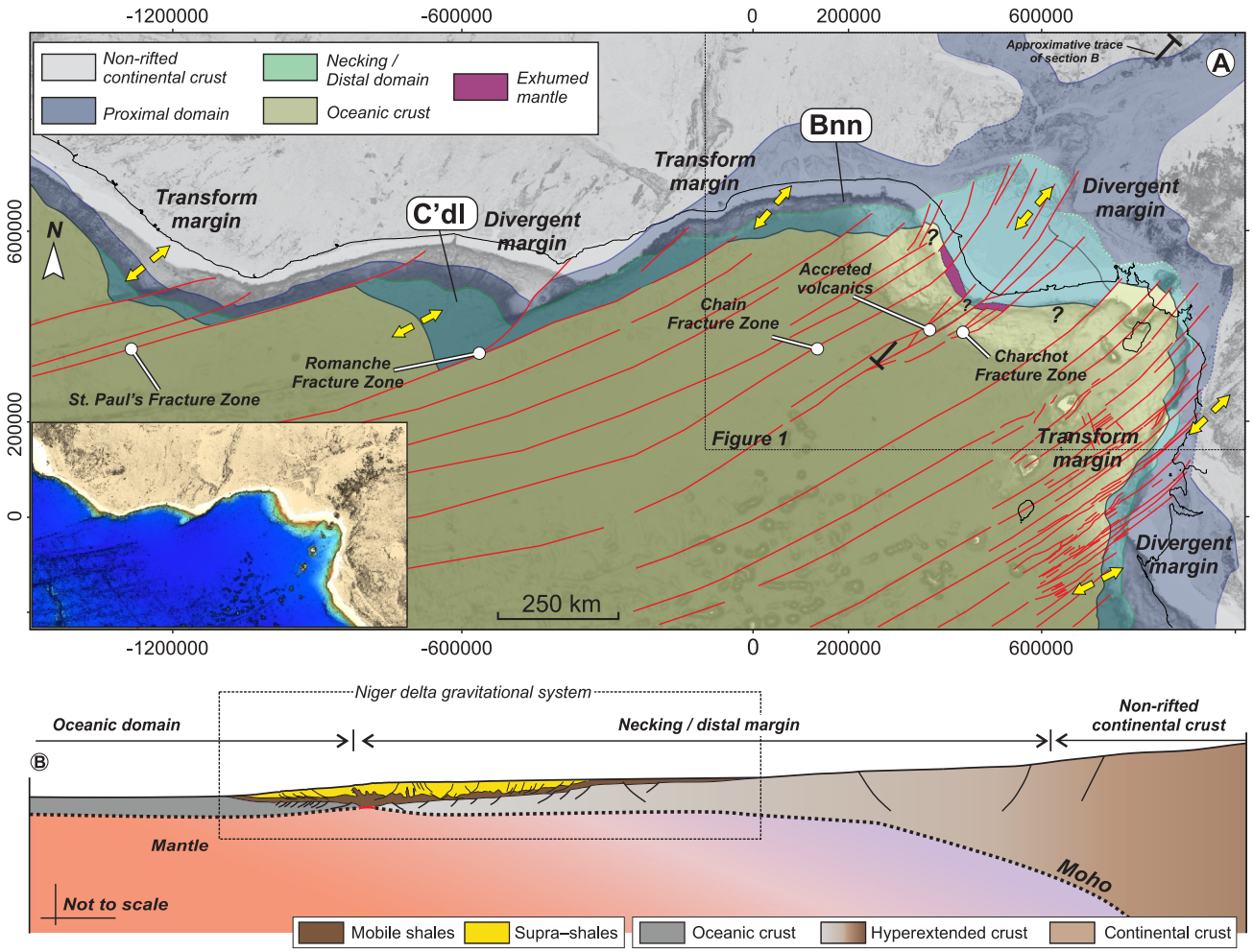

Figure 20. (a) Regional framework of the African passive margin, showing the different rift segments, their associated crustal domains, and the hyperextended domain. Yellow arrows indicate the direction of extension along the various rift segments. (b) Schematic crustal section illustrating the position of the Niger Delta gravitational system and the crustal domains of the divergent African passive margin. Abbreviations: Bnn, Benin Margin; C'dl, Cote d'Ivoire Margin.

10. Conclusions

Based on the interpretation of an extensive seismic data set, we studied the evolution, structural style, and timing of the deformation for the Niger Delta. This large shale-dominated sedimentary wedge is located on a divergent segment of the hyperextended African passive margin. The basement consists of oceanic crust in the present-day offshore region, passing landward to a thinned continental crust through an ocean-continent transition zone. The current configuration of the delta is the result of the progressive infilling, from the Early Miocene to the Pliocene, of two primary sub-basins separated by the Charcot fault zone. From the Pliocene onward, the basin became increasingly homogenized. Delta progradation over poorly consolidated Paleocene to Eocene sediments—primarily marine and pro-delta shales—led to the generation of overpressure conditions and to the downslope expulsion of mobile shales. Rapid burial and/or early hydrocarbon expulsion helped to create an overpressure regime in the Akata shales. The top of the overpressure was not constrained by lithological boundaries and migrated over time within the basin.

Shale mobilization and downslope flow led to the formation of shale ridges and walls, which are associated with asymmetric minibasins filled by growth strata of Lower Miocene to Quaternary sediments. In these minibasins, wedges of sediments thickening toward the landward-facing margin of the mobile shale highs have previously been interpreted as due to counterregional faulting. However, we propose that these features result instead from downslope flow of mobile shales, which drives asymmetric shale inflation.

Significant volumes of shales have accumulated above a zone where exhumed mantle has been interpreted. South of this region, shale mobility is reduced due to various factors, including a primary rheological boundary associated with a lithological change and buttressing effects associated with the occurrence of deep-seated structural features inherited from the passive margin. Gravity spreading induced extension in the updip region of the delta since the Paleogene; however, regional deformation is recorded basinward (i.e., within the transitional domain and the outer fold–thrust belt) only since the Late Miocene.

Restoration of regional cross sections demonstrates that the magnitude of updip extension is approximately double than the amount of shortening at the toe of the gravity-driven system. This indicates that transfer of the deformation toward the outer, basinward sector of the Niger delta involved tectonic (i.e., lateral) compaction and massive volume loss distributed across a thick shale section.

This study, besides confirming the fundamental role played by volume change in accommodating horizontal shortening in deepwater fold–thrust belts, provides new insights into the styles of deformation of thick mobile shales in delta systems and on the controls exerted by the pre-existing structures of the hyperextended continental margin. Our results provide a better understanding of the modes and timing of structural development in shale-dominated delta systems, beyond generic statements on the often invoked—but not always thoroughly investigated—controls exerted by the architecture of the continental margin and the ocean-continent transition zone on mobile shales.

Data Availability Statement

The seismic data used in this study are from PGS and TGS. The data supporting the interpretations and data products related to this paper are available in the online repository: Spina V. (2024). Supporting Information S1 and data set used in the study: Shale tectonics in the hyperextended continental margin of the Niger Delta [Dataset]. Figshare. https://doi.org/10.6084/m9.figshare.27316476.

Acknowledgments

The authors wish to thank TotalEnergies, SPDC (Shell Petroleum Development Company of Nigeria), PSG, and TGS for permission to publish the seismic data shown in this manuscript. The authors are also grateful to Getech for providing regional gravity and magnetic data and to Petroleum Experts Ltd. (Petex) for licensing the Move software. JIS also thanks the support of the Applied Geodynamics Laboratory (AGL) Industrial Associates program. An updated list of member companies of AGL is available at https://www.beg.utexas.edu/agl/sponsors. Publication authorized by the Director, Bureau of Economic Geology, The University of Texas at Austin. Restoration of cross sections was carried out with Move software from Petroleum Experts Ltd. (Petex). The authors wish to thank the editor and the anonymous reviewers for their constructive comments, which significantly improved the original version of the manuscript. Open access publishing facilitated by Universita degli Studi di Camerino, as part of the Wiley - CRUI-CARE agreement.

References

Adegoke, O. S., Oyebamiji, A. S., Edet, J. J., Osterloff, P. L., & Ulu, O. K. (2017). Chapter Geology of the Niger delta Basin. In O. S. Adegoke, A. S. Oyebamiji, J. J. Edet, P. L. Osterloff, & O. K. Ulu (Eds.), *Cenozoic foraminifera and calcareous nannofossil biostratigraphy of the Niger delta* (pp. 25–66). Elsevier. https://doi.org/10.1016/B978-0-12-812161-0.00002-8

Ajakaiye, D. E., & Bally, A. W. (2002). *Course manual and atlas of structural styles of reflection profiles from Niger delta, American Association of Petroleum Geologists Continuing Education Course Note Series* (Vol. 41, pp. 1–107). American Association of Petroleum Geologists.

Albertz, M., Beaumont, C., & Ings, S. J. (2009). Geodynamic modeling of sedimentation-induced overpressure, gravitational spreading, and deformation of passive margin mobile shale basins. In L. J. Wood (Ed.), *Shale Tectonics, American Association of Petroleum Geologists Memoir* (Vol. 93, pp. 29–62). American Association of Petroleum Geologists. https://doi.org/10.1306/13231307M933417

Allen, G. P., & Mercier, F. (1987). Les deltas: Sédimentologie et exploration pétrolière. *Bulletin de la Societe Geologique de France*, *3*(7), 1247–1269. https://doi.org/10.2113/gssgfbull.III.7.1247

Amogu, D. K., Filbrandt, J., Ladipo, K. O., Anowai, C., & Onuoha, K. (2011). Seismic interpretation, structural analysis, and fractal study of the Greater Ughelli Depobelt, Niger delta Basin, Nigeria. *The Leading Edge*, *30*(6), 640–648. https://doi.org/10.1190/1.3599149

Avbovbo, A. A. (1978). Tertiary lithostratigraphy of the Niger delta. *AAPG Bulletin*, *62*(2), 295–300. https://doi.org/10.1306/C1EA482E-16C9-11D7-8645000102C1865D

Benesh, N. P., Plesch, A., & Shaw, J. H. (2014). Geometry, kinematics, and displacement characteristics of tear-faults systems: An example from the deep-water Niger Delta. *AAPG Bulletin*, *98*(3), 465–482. https://doi.org/10.1306/06251311013

Benjamin, U. K., & Huuse, M. (2017). Seafloor and buried mounds on the western slope of the Niger Delta. *Marine and Petroleum Geology*, *83*, 158–173. https://doi.org/10.1016/j.marpetgeo.2017.02.023

Bilotti, F., & Shaw, J. H. (2005). Deep-water Niger Delta fold and thrust belt modeled as a critical-taper wedge: The influence of elevated basal fluid pressure on structural styles. *AAPG Bulletin*, *89*(11), 1475–1491. https://doi.org/10.1306/06130505002

Briggs, S. E., Cartwright, J., & Davies, R. J. (2009). Crustal structure of the deepwater west Niger Delta passive margin from the interpretation of seismic reflection data. *Marine and Petroleum Geology*, *26*(6), 936–950. https://doi.org/10.1016/j.marpetgeo.2008.07.003

Briggs, S. E., Davies, R. J., Cartwright, J. A., & Morgan, R. (2006). Multiple detachment levels and their control on fold styles in the compressional domain of the deepwater west Niger Delta. *Basin Research*, *18*(4), 435–450. https://doi.org/10.1111/j.1365-2117.2006.00300.x

Brown, K. M. (1990). The nature and hydrogeologic significance of mud diapirs and diatremes for accretionary systems. *Journal of Geophysical Research*, *95*(B6), 8969–8982. https://doi.org/10.1029/JB095iB06p08969

Brun, J.-P., & Fort, X. (2011). Salt tectonics at passive margins: Geology versus models. *Marine and Petroleum Geology*, *28*(6), 1123–1145. https://doi.org/10.1016/j.marpetgeo.2011.03.004

Brun, J. P., & Fort, X. (2018). Growth of continental shelves at salt margins. *Frontiers in Earth Science*, *6*, 209. https://doi.org/10.3389/feart.2018.00209

Brun, J.-P., & Mauduit, T. P.-O. (2008). Rollovers in salt tectonics: The inadequacy of the listric fault model. *Tectonophysics*, *457*(1–2), 1–11. https://doi.org/10.1016/j.tecto.2007.11.038

Brune, S., Popov, A. A., & Sobolev, S. V. (2012). Modeling suggests that oblique extension facilitates rifting and continental break-up. *Journal of Geophysical Research*, *117*(B8), B08402. https://doi.org/10.1029/2011JB008860

Burke, K. (1972). Longshore drift, submarine canyons, and submarine fans in development of Niger Delta. *AAPG Bulletin*, *56*(10), 1975–1983. https://doi.org/10.1306/819A41A2-16C5-11D7-8645000102C1865D

Burke, K., Dessauvagie, T. F. J., & Whiteman, A. J. (1971). Opening of the Gulf of Guinea and geological history of the Benue Depression and Niger Delta. *Nature; Physical Science*, *233*(38), 51–55. https://doi.org/10.1038/physci233051a0

Bustin, R. M. (1988). Sedimentology and characteristics of dispersed organic matter in Tertiary Niger Delta: Origin of source rocks in a deltaic environment. *AAPG Bulletin*, *72*(3), 277–298. https://doi.org/10.1306/703C8C18-1707-11D7-8645000102C1865D

Butler, R. W. H., Bond, C., Cooper, M. A., & Watkins, H. (2019). Fold-thrust structures-where have all the buckles gone? In C. E. Bond, & H. D. Lebit (Eds.), *Folding and Fracturing of Rocks: 50 Years of Research since the Seminal Text Book of J. G. Ramsay, Geological Society of London, Special Publications* (Vol. 487(1), pp. 21–44). : Geological Society of London. https://doi.org/10.1144/SP487.7

Butler, R. W. H., & Paton, C. (2010). Evaluating lateral compaction in deepwater fold and thrust belts: How much are we missing from "nature's sandbox". *Geological Society of America Today*, *20*(3), 4–10. https://doi.org/10.1130/GSATG77A.1

Cande, S. C., & Kent, D. V. (1995). Revised calibration of the geomagnetic polarity timescale for the Late Cretaceous and Cenozoic. *Journal of Geophysical Research*, *100*(B4), 6093–6095. https://doi.org/10.1029/94JB03098

Carboni, F., Back, S., & Barchi, M. R. (2018). Application of the ADS method to predict a "hidden" basal detachment: NW Borneo fold-and-thrust belt. *Journal of Structural Geology*, *118*, 210–223. https://doi.org/10.1016/j.jsg.2018.10.011

Chapman, R. E. (1994). The geology of abnormal pore pressures. In W. H. Fertl, R. E. Chapman, & R. F. Hotz (Eds.), *Studies in Abnormal Pressures. Developments in Petroleum Science* (Vol. 38, pp. 19–49). Elsevier. https://doi.org/10.1016/S0376-7361(09)70226-2

Chima, K. I., Do Couto, D., Leroux, E., Gardin, S., Hoggmascall, N., Rabineau, M., et al. (2019). Seismic stratigraphy and depositional architecture of Neogene intraslope basins, offshore Niger Delta. *Marine and Petroleum Geology*, *109*, 449–468. https://doi.org/10.1016/j.marpetgeo.2019.06.030

Chima, K. I., Granjeon, D., Do Couto, D., Leroux, E., Gorini, C., Rabineau, M., et al. (2021). Tectono-stratigraphic evolution of the offshore western Niger delta from the Cretaceous to present: Implications of delta dynamics and paleo-topography on the gravity-driven deformation. *Basin Research*, *34*(1), 25–49. https://doi.org/10.1111/bre.12609

Choubert, G., & Faure-Muret, A. (1990). *International geological map of Africa (3rd ed., 6 sheets, scale 1/5,000,000)*. Commission for the Geological Map of the World (CCGM) and UNESCO.

Cobbold, P. R., Clarke, B. J., & Løseth, H. (2009). Structural consequences of fluid overpressure and seepage forces in the outer thrust belt of the Niger Delta. *Petroleum Geoscience*, *15*(1), 3–15. https://doi.org/10.1144/1354-079309-784

Cobbold, P. R., & Szatmari, P. (1991). Radial gravitational gliding on passive margins. *Tectonophysics*, *188*(3–4), 249–289. https://doi.org/10.1016/0040-1951(91)90459-6

Cohen, H. A., & McClay, K. (1996). Sedimentation and shale tectonics of the northwestern Niger Delta front. *Marine and Petroleum Geology*, *13*(3), 313–328. https://doi.org/10.1016/0264-8172(95)00067-4

Connors, C. D., Denson, D. B., Kristiansen, G., & Angstadt, D. M. (1998). Compressive anticlines of the mid-outer slope, central Niger Delta. *AAPG Bulletin*, *82*(10), 1903.

Corredor, F., Shaw, J. H., & Bilotti, F. (2005). Structural styles in the deep-water fold and thrust belts of the Niger Delta. *AAPG Bulletin*, *89*(6), 753–780. https://doi.org/10.1306/02170504074

Cramez, C., & Jackson, M. P. A. (2000). Superposed deformation straddling the continental-oceanic transition in deep-water Angola. *Marine and Petroleum Geology*, *17*(10), 1095–1109. https://doi.org/10.1016/S0264-8172(00)00053-2

Crans, W., & Mandl, G. (1981). On the theory of growth faulting part II (b): Genesis of the "unit". *Journal of Petroleum Geology*, *3*(3), 333–355. https://doi.org/10.1111/j.1747-5457.1981.tb00935.x

Crans, W., Mandl, G., & Haremboure, J. (1980). On the theory of growth faulting: A geomechanical delta model based on gravity sliding. *Journal of Petroleum Geology*, *2*(3), 265–307. https://doi.org/10.1111/j.1747-5457.1980.tb00707.x

Dailly, G. C. (1976). A possible mechanism relating progradation, growth faulting, clay diapirism and overthrusting in a regressive sequence of sediments. *Bulletin of Canadian Petroleum Geology*, *24*(1), 92–116. https://doi.org/10.35767/gscpgbull.24.1.092

Damuth, J. E. (1994). Neogene gravity tectonics and depositional processes on the deep Niger Delta continental margin. *Marine and Petroleum Geology*, *11*(3), 321–346. https://doi.org/10.1016/0264-8172(94)90053-1

Davies, R. J., MacLeod, C. J., Morgan, R., & Briggs, S. E. (2005). Termination of a fossil continent-ocean fracture zone imaged with three-dimensional seismic data: The Chain Fracture Zone, eastern equatorial Atlantic. *Geology*, *33*(8), 641–644. https://doi.org/10.1130/G21530.1

Day-Stirrat, R. J., McDonnell, A., & Wood, L. J. (2010). Diagenetic and seismic concerns associated with interpretation of deeply buried mobile shales. In L. J. Wood (Ed.), *Shale Tectonics, American Association of Petroleum Geologists Memoir* (Vol. 93, pp. 5–27). American Association of Petroleum Geologists. https://doi.org/10.1306/13231306M93730

Dean, S., Morgan, J., & Brandeburg, J. P. (2015). Influence of mobile shale on thrust faults: Insights from discrete element simulations. *AAPG Bulletin*, *99*(3), 403–432. https://doi.org/10.1306/10081414003

Deptuck, M. E., Sylvester, Z., Pirmez, C., & O'Byrne, C. (2007). Migration–aggradation history and 3-D seismic geomorphology of submarine channels in the Pleistocene Benin-major Canyon, western Niger Delta slope. *Marine and Petroleum Geology*, *24*(6–9), 406–433. https://doi.org/10.1016/j.marpetgeo.2007.01.005

Diab, A. I., Sanuade, O., & Radwan, A. E. (2023). An integrated source rock potential, sequence stratigraphy, and petroleum geology of (Agbada-Akata) sediment succession, Niger delta: Application of well logs aided by 3D seismic and basin modeling. *Journal of Petroleum Exploration and Production Technology*, *13*(1), 237–257. https://doi.org/10.1007/s13202-022-01548-4

Diegel, F. A., Karlo, J. F., Schuster, D. C., Shoup, R. C., & Tauvers, P. R. (1995). Cenozoic structural evolution and tectono-stratigraphic framework of the northern Gulf Coast continental margin. In M. P. A. Jackson, D. G. Roberts, & S. Snelson (Eds.), *Salt Tectonics: A Global Perspective, American Association of Petroleum Geologists Memoir* (Vol. 65, pp. 109–151). American Association of Petroleum Geologists. https://doi.org/10.1306/M65604C6

Dooley, T. P., Hudec, M. R., Pichel, L. M., & Jackson, M. P. (2020). The impact of base-salt relief on salt flow and suprasalt deformation patterns at the autochthonous, paraautochthonous and allochthonous level: Insights from physical models. In K. R. McClay, & J. Hammerstein (Eds.), *Passive Margins: Tectonics, Sedimentation and Magmatism, Geological Society of London, Special Publications* (Vol. 476(1), pp. 287–315). : Geological Society of London. https://doi.org/10.1144/SP476.13

Dooley, T. P., Jackson, M. P., & Hudec, M. R. (2007). Initiation and growth of salt-based thrust belts on passive margins: Results from physical models. *Basin Research*, *19*(1), 165–177. https://doi.org/10.1111/j.1365-2117.2007.00317.x

Dooley, T. P., Jackson, M. P., & Hudec, M. R. (2022). Growth and evolution of salt canopies on a salt-detached slope: Insights from physical models. *AAPG Bulletin*, *107*(12), 2053–2059. https://doi.org/10.1306/08072222013

Dooley, T. P., Soto, J. I., Reber, J. E., Hudec, M. R., Peel, F. J., & Apps, G. M. (2024). Modeling mobile shales under contraction: Critical analyses of new analog simulations of shale tectonics and comparison with salt-bearing systems. *Interpretation*, *12*(4), SF17–SF38. https://doi.org/10.1190/INT-2024-0025.1

Doré, T., & Lundin, E. (2015). Hyperextended continental margins-knowns and unknowns. *Geology*, *43*(1), 95–96. https://doi.org/10.1130/focus012015.1

Doust, H., & Omatsola, E. (1990). Niger delta. In J. D. Edwards & P. A. Santogrossi (Eds.), *Divergent/Passive Margin Basins, American Association of Petroleum Geologists Memoir* (Vol. 48, pp. 201–238). American Association of Petroleum Geologists. https://doi.org/10.1306/ce41915c3

Dupuis, M., Imbert, P., Odonne, F., & Vendeville, B. (2019). Mud volcanism by repeated roof collapse: 3D architecture and evolution of a mud volcano cluster offshore Nigeria. *Marine and Petroleum Geology*, *110*, 368–387. https://doi.org/10.1016/j.marpetgeo.2019.07.033

Ekweozor, C. M., & Daukoru, E. M. (1994). Northern delta depobelt portion of the Akata–Agbada (!) petroleum system, Niger Delta, Nigeria. In L. B. Magoon & W. G. Dow (Eds.), *The Petroleum System—From Source to Trap, American Association of Petroleum Geologists Memoir* (Vol. 60, pp. 599–613). American Association of Petroleum Geologists. https://doi.org/10.1306/M60585C36

Espurt, N., Callot, J. P., Totterdell, J., Struckmeyer, H., & Vially, R. (2009). Interactions between continental breakup dynamics and large-scale delta system evolution: Insights from the Cretaceous Ceduna delta system, Bight Basin, Southern Australian margin. *Tectonics*, *28*(6), TC6002. https://doi.org/10.1029/2009TC002447

Evamy, B. D., Haremboure, J., Kamerling, P., Knaap, W. A., Molloy, F. A., & Rowlands, P. H. (1978). Hydrocarbon habitat of Tertiary Niger Delta. *AAPG Bulletin*, *62*(1), 1–39. https://doi.org/10.1306/C1EA47ED-16C9-11D7-8645000102C1865D

Fairhead, J. D., & Binks, R. M. (1991). Differential opening of the Central and South Atlantic oceans and the opening of the West African rift system. *Tectonophysics*, *187*(1–3), 191–203. https://doi.org/10.1016/0040-1951(91)90419-S

Flemings, P. B. (2021). *A concise guide to overpressure: Origins, predictions, and applications*. Cambridge University Press.

Fort, X., Brun, J.-P., & Chauvel, F. (2004). Salt tectonics on the Angolan margin, synsedimentary deformation processes. *AAPG Bulletin*, *88*(11), 1523–1544. https://doi.org/10.1306/06010403012

Galloway, W. E. (1986). Growth faults and fault–related structures of prograding terrigenous clastic continental margins. *Gulf Coast Association of Geological Societies Transactions*, *36*, 121–128.

Ge, Z., Rosenau, M., Warsitzka, M., & Gawthorpe, R. L. (2019). Overprinting translational domains in passive margin salt basins: Insights from analogue modelling. *Solid Earth*, *10*(4), 1283–1300. https://doi.org/10.5194/se-10-1283-2019

GEBCO. (2023). The global bathymetric chart of the oceans-bathymetric compilation group 2023 (GEBCO_2023 Grid)–A continuous terrain model of the global oceans and land [Dataset]. *British Oceanographic Data Centre, National Oceanography Centre, Natural Environment Research Council [NERC]*. https://download.gebco.net/

GEBCO. (2024). Undersea feature names gazetteer [Dataset]. https://www.ngdc.noaa.gov/gazetteer/

Geoffroy, L. (2005). Volcanic passive margins. *Comptes Rendus Geoscience*, *337*(16), 1395–1408. https://doi.org/10.1016/j.crte.2005.10.006

Granado, P., Santolaria, P., & Muñoz, J. A. (2023). Interplay of downbuilding and gliding in salt-bearing rifted margins: Insights from analogue modeling and natural case studies. *AAPG Bulletin*, *107*(12), 2091–2118. https://doi.org/10.1306/08072221203

Graue, K. (2000). Mud volcanoes in deepwater Nigeria. *Marine and Petroleum Geology*, *17*(8), 954–974. https://doi.org/10.1016/S0264-8172(00)00016-7

Haack, R. C., Sudararaman, P., Diedjonmahor, J. O., Hongbin, X., Gant, N. J., May, E. D., & Kelsch, K. (2000). Niger delta petroleum systems, Nigeria. In M. R. Mello & B. J. Katz (Eds.), *Petroleum systems of South Atlantic margins, American Association of Petroleum Geologists Memoir* (Vol. 73, pp. 213–231). American Association of Petroleum Geologists.

Harkins, K. L., & Baugher, J. W. III. (1968). Geological significance of abnormal formation pressures. *Journal of Petroleum Technology*, *21*(8), 961–966. https://doi.org/10.2118/2228-PA

Heine, C., Zoethout, J., & Muller, R. D. (2013). Kinematics of the South Atlantic rift. *Solid Earth*, *4*(2), 215–253. https://doi.org/10.5194/se-4-215-2013

Heiniö, P., & Davies, R. J. (2006). Degradation of compressional fold belts: Deep-water Niger delta. *AAPG Bulletin*, *90*(5), 753–770. https://doi.org/10.1306/11210505090

Higgins, S., Clarke, B., Davies, R. J., & Cartwrigth, J. A. (2009). Internal geometry and growth history of a thrust-related anticline in a deep-water fold belt. *Journal of Structural Geology*, *31*(12), 1597–1611. https://doi.org/10.1016/j.jsg.2009.07.006

Hooper, R. J., Fitzsimmons, R. J., Neil, G., & Vendeville, B. C. (2002). The role of deformation in controlling depositional patterns in the south-central Niger Delta, West Africa. *Journal of Structural Geology*, *24*(4), 847–859. https://doi.org/10.1016/S0191-8141(01)00122-5

Hopper, J. R., Funck, T., Tucholke, B. E., Larsen, H. C., Holbrook, W. S., Louden, K. E., et al. (2004). Continental breakup and the onset of ultra-slow seafloor spreading off Flemish Cap on the Newfoundland rifted margin. *Geology*, *32*(1), 93–96. https://doi.org/10.1130/G19694.1

Hospers, J. (1971). The geology of the Niger Delta area. In F. M. Delany (Ed.), *The Geology of the East Atlantic Continental Margin – 4 Africa (Report No. 70/16)* (pp. 121–142). Institute of Geological Sciences.

Hudec, M. R., Dooley, T. P., Peel, F. J., & Soto, J. I. (2020). Controls on the evolution of passive–margin salt basins: Structure and evolution of the Salina del Bravo region, northeastern Mexico. *GSA Bulletin*, *132*(5–6), 997–1012. https://doi.org/10.1130/B35283.1

Hudec, M. R., & Jackson, M. P. (2007). Terra infirma: Understanding salt tectonics. *Earth-Science Reviews*, *82*(1–2), 1–28. https://doi.org/10.1016/j.earscirev.2007.01.001

Hudec, M. R., Norton, I. O., Jackson, M. P., & Peel, F. J. (2013). Jurassic evolution of the Gulf of Mexico salt basin. *AAPG Bulletin*, *97*(10), 1683–1710. https://doi.org/10.1306/04011312073

Hudec, M. R., & Soto, J. I. (2021). Piercement mechanisms for mobile shales. *Basin Research*, *33*(5), 2862–2882. https://doi.org/10.1111/bre.12586

Ings, S. J., & Beaumont, C. (2010). Continental margin shale tectonics: Preliminary results from coupled fluid-mechanical models of large-scale delta instability. *Journal of the Geological Society*, *167*(3), 571–582. https://doi.org/10.1144/0016-76492009-052

Jackson, M. P., & Galloway, W. E. (1984). Thin–skinned gravity sliding as a mechanism for growth faulting: Unit 10: Principles. In M. P. Jackson & W. E. Galloway (Eds.), *Structural and depositional styles of Gulf Coast tertiary continental margins: Application to hydrocarbon exploration, American Association of Petroleum Geologists Special Volumes, Courses Notes* (Vol. 25, pp. 37–45). American Association of Petroleum Geologists.

Jackson, M. P., & Hudec, M. R. (2017). *Salt tectonics: Principles and practice*. Cambridge University Press. https://doi.org/10.1017/9781139003988

Jackson, M. P. A., Vendeville, B. C., & Schultz-Ela, D. D. (1994). Structural dynamics of salt systems. *Annual Review of Earth and Planetary Sciences*, *22*(1), 93–117. https://doi.org/10.1146/annurev.ea.22.050194.000521

Jacques, J. M., Parsons, M. E., Price, A. D., & Schwartz, D. M. (2003). Improving geologic understanding with gravity and magnetic data: Examples from Gabon, Nigeria and the Gulf of Mexico. *First Break*, *21*(11), 57–62. https://doi.org/10.3997/1365-2397.21.11.25674

Jolly, B. A., Lonergan, L., & Whittaker, A. C. (2016). Growth history of fault-related folds and interaction with seabed channels in the toe-thrust region of the deep-water Niger delta. *Marine and Petroleum Geology*, *70*, 58–76. https://doi.org/10.1016/j.marpetgeo.2015.11.003

King, R. C., Backé, G., Morley, C. K., Hillis, R. R., & Tingay, M. R. (2010). Balancing deformation in NW Borneo: Quantifying plate–scale vs. gravitational tectonics in a delta and deepwater fold–thrust belt system. *Marine and Petroleum Geology*, *27*(1), 238–246. https://doi.org/10.1016/j.marpetgeo.2009.07.008

Knox, G. J., & Omatsola, E. M. (1989). Development of the Cenozoic Niger delta in terms of the escalator regression model and impact on hydrocarbon distribution. In W. J. M. van der Linden, S. A. P. L. Cloetingh, J. P. K. Kaasschieter, W. J. E. van de Graaff, J. Vandenberghe, & J. A. M. van der Gun (Eds.), *Proceedings KNGMG Symposium "Coastal Lowlands, Geology and Geotechnology"* (pp. 181–202). Kluwer Academic Publishers.

Kopf, A. J. (2002). Significance of mud volcanism. *Reviews of Geophysics*, *40*(2), 2-1–2-52. https://doi.org/10.1029/2000RG000093

Krueger, S. W., & Grant, N. T. (2011). The growth history of toe thrusts of the Niger delta and the role of pore pressure. In K. McClay, J. Shaw, & J. Suppe (Eds.), *Thrust fault-related folding, American Association of Petroleum Geologists Memoir* (Vol. 94, pp. 357–390). American Association of Petroleum Geologists. https://doi.org/10.1306/13251345M943435

Lacoste, A., Vendeville, B. C., Mourgues, R., Loncke, L., & Lebacq, M. (2012). Gravitational instabilities triggered by fluid overpressure and downslope incision–insights from analytical and analogue modelling. *Journal of Structural Geology*, *42*, 151–162. https://doi.org/10.1016/j.jsg.2012.05.011

Larberg, G. M. B. (1983). Contra-regional faulting: Salt withdrawal compensation, offshore Louisiana, Gulf of Mexico. In A. W. Bally (Ed.), *Seismic expression of structural styles: A picture and work Atlas, American Association of Petroleum Geologists Studies in Geology* (Vol. 15, pp. 2.3.2-42–2.3.2-43). American Association of Petroleum Geologists.

Leduc, A. M., Davies, R. J., Densmore, A. L., & Imber, J. (2012). The lateral strike-slip domain in gravitational detachment delta systems: A case study of the northwestern margin of the Niger Delta. *AAPG Bulletin*, *96*(4), 709–728. https://doi.org/10.1306/09141111035

Lehner, F. K. (1999). Approximate theory of substratum creep and associated overburden deformation in salt basins and deltas. In F. K. Lehner & J. L. Urai (Eds.), *Aspects of tectonic faulting: In Honour of Georg Mandl* (pp. 21–47). Springer.

Lehner, P., & De Ruiter, P. A. C. (1977). Structural history of Atlantic margin of Africa. *AAPG Bulletin*, *61*(7), 961–981. https://doi.org/10.1306/C1EA43B0-16C9-11D7-8645000102C1865D

Le Pourhiet, L., May, D. A., Huile, L., Watremez, L., & Leroy, S. (2017). A genetic link between transform and hyper-extend margins. *Earth Planetary Sciences Letters*, *465*, 184–192. https://doi.org/10.1016/j.epsl.2017.02.043

MacGregor, D. S., Robinson, J., & Spear, G. (2003). Play fairways of the Gulf of Guinea transform margin. In T. Arthur, D. S. MacGregor, & N. R. Cameron (Eds.), *Petroleum Geology of Africa: New Themes and Developing Technologies* (Vol. 207(1), pp. 131–150). : Geological Society of London, Special Publications. https://doi.org/10.1144/GSL.SP.2003.207.7

Magbagbeola, O. A., & Willis, B. J. (2007). Sequence stratigraphy and syndepositional deformation of the Agbada Formation, Robertkiri field, Niger Delta, Nigeria. *AAPG Bulletin*, *91*(7), 945–958. https://doi.org/10.1306/02050705150

Maloney, D., Davies, R., Imber, J., Higgins, S., & King, S. (2010). New insights into deformation mechanisms in the gravitationally driven Niger Delta deep-water fold and thrust belt. *AAPG Bulletin*, *94*(9), 1401–1424. https://doi.org/10.1306/01051009080

Manatschal, G. (2004). New models for evolution of magma-poor rifted margins based on a review of data and concepts from West Iberia and the Alps. *International Journal of Earth Sciences*, *93*(3), 432–466. https://doi.org/10.1007/s00531-004-0394-7

Mascle, J., Marhino, M., & Wanesson, J. (1986). The structure of the Guinean continental margin: Implications for the connections between the Central and South Atlantic Oceans. *Geologische Rundschau*, *75*, 57–70. https://doi.org/10.1007/BF01770178

Mascle, J. R., Bornhold, B. D., & Renard, V. (1973). Diapiric structures off Niger Delta. *AAPG Bulletin*, *57*(9), 1672–1678. https://doi.org/10.1306/83D91029-16C7-11D7-8645000102C1865D

Maudit, T., Guerin, G., Brun, J.-P., & Lecanu, H. (1997). Raft tectonics: The effects of basal slope angle and sedimentation rate on progressive extension. *Journal of Structural Geology*, *19*(9), 1219–1230. https://doi.org/10.1016/S0191-8141(97)00037-0

McClay, K., Dooley, T., & Zamora, G. (2003). Analogue models of delta systems above ductile substrates. In P. Van Rensbergen, R. R. Hillis, A. J. Maltman, & C. K. Morley (Eds.), *Subsurface Sediment Mobilization, Geological Society of London, Special Publications* (Vol. 216(1), pp. 411–428). : Geological Society of London. https://doi.org/10.1144/GSL.SP.2003.216.01.27

McClay, K. R., Dooley, T., & Lewis, G. (1998). Analog modeling of progradational delta systems. *Geology*, *26*(9), 771–774. https://doi.org/10.1130/0091–7613(1998)026<0771:AMOPDS>2.3.CO;2

Mercier de Lépinay, M., Loncke, L., Basile, C., Roest, W. R., Patriat, M., Maillard, A., & De Clarens, P. (2016). Transform continental margins-Part 2: A worldwide review. *Tectonophysics*, *693*(A), 96–115. https://doi.org/10.1016/j.tecto.2016.05.038

Merki, P. (1972). Structural geology of the Cenozoic Niger Delta. In T. F. J. Dessauvagie & A. J. Whiteman (Eds.), *Proceedings of the Conference on African Geology, Held at the University of Ibadan from 7-14 December 1970 in the Commemoration of the Tenth Anniversary of the Founding of the Geology Department* (pp. 635–646). Department of Geology, University of Ibadan.

Morency, C., Huismans, R. S., Beaumont, C., & Fullsack, P. (2007). A numerical model for coupled fluid flow and matrix deformation with applications to disequilibrium compaction and delta stability. *Journal of Geophysical Research*, *112*(B10), B10407. https://doi.org/10.1029/2006JB004701

Morgan, R. (2003). Prospectivity in ultradeep water: The case for petroleum generation and migration within the outer parts of the Niger delta apron. In T. Arthur, D. S. MacGregor, & N. R. Cameron (Eds.), *Petroleum Geology of Africa: New Themes and Developing Technologies, Geological Society of London, Special Publications* (Vol. 207(1), pp. 45–51). Geological Society of London. https://doi.org/10.1144/GSL.SP.2003.207.8

Morley, C. K. (2003). Mobile shale related deformation in large deltas developed on passive and active margins. In P. Van Rensbergen, R. R. Hillis, A. J. Maltman, & C. K. Morley (Eds.), *Subsurface Sediment Mobilization, Geological Society of London, Special Publications* (Vol. 216(1), pp. 335–357). Geological Society of London. https://doi.org/10.1144/GSL.SP.2003.216.01.22

Morley, C. K., & Guerin, G. (1996). Comparison of gravity-driven deformation styles and behaviour associated with mobile shales and salt. *Tectonics*, *15*(6), 1154–1170. https://doi.org/10.1029/96TC01416

Morley, C. K., King, R., Hillis, R., Tingay, M., & Backe, G. (2011). Deepwater fold and thrust belt classification, tectonics, structure and hydrocarbon prospectivity: A review. *Earth-Science Reviews*, *104*(1–3), 41–91. https://doi.org/10.1016/j.earscirev.2010.09.010

Morley, C. K., Promrak, W., Apuanram, W., Chaiyo, P., Chantraprasert, S., Ong, D., et al. (2023). A major Miocene deepwater mud canopy system: The North Sabah–Pagasa Wedge, northwestern Borneo. *Geosphere*, *19*(1), 291–334. https://doi.org/10.1130/GES02518.1

Morley, C. K., Tingay, M., Hillis, R., & King, R. (2008). Relationships between structural style, overpressures, and modern stress, Baram Delta Province, Northwest Borneo. *Journal of Geophysical Research: Solid Earth*, *113*(B9), B09410. https://doi.org/10.1029/2007JB005324

Morley, C. K., von Hagke, C., Hansberry, R. L., Collins, A. S., Kanitpanyacharoen, W., & King, R. (2017). Review of major shale–dominated detachment and thrust characteristics in the diagenetic zone: Part I, meso–and macro–scopic scale. *Earth-Science Reviews*, *173*, 168–228. https://doi.org/10.1016/j.earscirev.2017.07.019

Mourgues, R., & Cobbold, P. R. (2006). Sandbox experiments on gravitational spreading and gliding in the presence of fluid overpressures. *Journal of Structural Geology*, *28*(5), 887–901. https://doi.org/10.1016/j.jsg.2005.12.013

Mourgues, R., Lecomte, E., Vendeville, B., & Raillard, S. (2009). An experimental investigation of gravity-driven shale tectonics in progradational delta. *Tectonophysics*, *474*(3–4), 643–656. https://doi.org/10.1016/j.tecto.2009.05.003

Musa, O. K., Kurowska, E., Schoeneich, K., & Alagbe, S. A. (2014). Mud volcanoes on the dry land of Nigeria. *Africa Geoscience Review*, *21*(1), 15–22.

Musa, O. K., Kurowska, E. E., Schoeneich, K., Solomon, A., Alagbe, S., & Ayok, J. (2016). Tectonic control on the distribution of onshore mud volcanoes in parts of the Upper Benue Trough, northeastern Nigeria. *Contemporary Trends in Geoscience*, *5*(1), 28–45. https://doi.org/10.1515/ctg-2016-0003

NOAA. (2022). ETOPO 2022 15 arc-second global relief model [Dataset]. *NOAA National Centers for Environmental Information*. https://doi.org/10.25921/fd45-gt74

Nwozor, K. K., Onuorah, L. O., Onyekuru, S. O., & Egbuachor, C. J. (2017). Calibration of Gardner coefficient for density–velocity relationships of Tertiary sediments in Niger Delta Basin. *Journal of Petroleum Exploration and Production Technology*, *7*(3), 627–635. https://doi.org/10.1007/s13202-017-0313-7

Obaja, N. G. (2009). Lecture Notes in Earth Sciences. *Geology and Mineral Resources of Nigeria*. (Vol. 120). Springer-Verlag.

Ogawa, K., & Back, S. (2022). Deepwater fold-thrust belt contraction driven by mixed deformation components. *Tectonophysics*, *841*, 229574. https://doi.org/10.1016/j.tecto.2022.229574

Ogbe, O. B. (2020). Sequence stratigraphic controls on reservoir characterization and architectural analysis: A case study of Tovo field, coastal swamp depobelt, Niger Delta Basin, Nigeria. *Marine and Petroleum Geology*, *121*, 104579. https://doi.org/10.1016/j.marpetgeo.2020.104579

Ogg, J. G. (2020). Geomagnetic polarity time scale. In F. M. Gradstein, J. G. Ogg, M. Schmitz, & G. Ogg (Eds.), *Geological Time Scale 2020* (pp. 159–192). Elsevier. https://doi.org/10.1016/B978-0-12-824360-2.00005-X

Oguadinma, V. O., Reynaud, J. Y., Delhaye-Prat, V., Akpi, T., Thackrey, S., Lanisa, A., & Dall'Asta, M. (2024). Gravity tectonics controls on reservoir-scale sandbodies: Insights from 3D seismic geomorphology of the canyons buried in the upper slope of the Eastern Niger Delta basin. *Energy Geoscience*, *5*(3), 100293. https://doi.org/10.1016/j.engeos.2024.100293

Oliveira, M. J. R., Zalán, P. V., Caldeira, J. L., Tanaka, A., Santarem, P., Trosdtorf, I., & Moraes, A. (2012). Linked extensional-compressional tectonics in gravitational systems in the Equatorial Margin of Brazil. In D. Gao (Ed.), *Tectonics and Sedimentation: Implications for Petroleum Systems, American Association of Petroleum Geologists Memoir* (Vol. 100, pp. 159–178). American Association of Petroleum Geologists. https://doi.org/10.1306/13351552M1003532

Onuoha, K. M. (1999). Structural features of Nigeria's coastal margin: An assessment base of age data from wells. *Journal of African Earth Sciences*, *29*(3), 485–499. https://doi.org/10.1016/S0899-5362(99)00111-6

Osborne, M. J., & Swarbrick, R. E. (1997). Mechanisms for generating overpressure in sedimentary basins: A reevaluation. *AAPG Bulletin*, *81*(6), 1023–1041. https://doi.org/10.1306/522B49C9-1727-11D7-8645000102C1865D

Pizzi, M., Lonergan, L., Whittaker, C., & Mayall, M. (2020). Growth of a thrust fault array in space and in time: An example from the deep-water Niger delta. *Journal of Structural Geology*, *137*, 104088. https://doi.org/10.1016/j.jsg.2020.104088

Rabineau, M., Leroux, E., Aslanian, D., Bache, F., Gorini, C., Moulin, M., et al. (2014). Quantifying subsidence and isostatic readjustment using sedimentary paleomarkers, example from the Gulf of Lion. *Earth and Planetary Science Letters*, *388*, 353–366. https://doi.org/10.1016/j.epsl.2013.11.059

Reijers, T. J. A., Petters, S. W., & Nwajide, C. S. (1997). The Niger Delta basin. In R. C. Selley (Ed.), *African basins. Sedimentary basins of the World* (Vol. 3, pp. 151–172). Elsevier Science. https://doi.org/10.1016/s1874-5997(97)80010-x

Restrepo-Pace, P. A. (2020). "Ductile Brittle" – Alternative structural interpretations for the Niger delta. In K. R. McClay, & J. A. Hammerstein (Eds.), *Passive Margins: Tectonics, Sedimentation and Magmatism, Geological Society of London, Special Publications* (Vol. 476(1), pp. 193–204). Geological Society of London. https://doi.org/10.1144/SP476.2

Rouby, D., Nalpas, T., Jermannaud, P., Robin, C., Guillocheau, F., & Raillard, S. (2011). Gravity driven deformation controlled by the migration of the delta front: The Plio-Pleistocene of the Eastern Niger delta. *Tectonophysics*, *513*(1–4), 54–67. https://doi.org/10.1016/j.tecto.2011.09.026

Rowan, M. G. (2020). Salt- and shale-detached gravity-driven failure of continental margins. In N. Scarselli, J. Adam, & D. Chiarella (Eds.), *Regional geology and tectonics: Principles of geologic analysis* (2nd ed.1, pp. 205–234). Elsevier. https://doi.org/10.1016/B978-0-444-64134-2.00010-9

Rowan, M. G., & Giles, K. A. (2021). Passive versus active salt diapirism. *AAPG Bulletin*, *105*(1), 53–63. https://doi.org/10.1306/05212020001

Rowan, M. G., Peel, F. J., & Vendeville, B. C. (2004). Gravity-driven fold belts on passive margins. In K. R. McClay (Ed.), *Thrust Tectonics and Hydrocarbon Systems, American Association of Petroleum Geologists Memoir* (Vol. 82, pp. 157–182). American Association of Petroleum Geologists.

Rowan, M. G., & Ratliff, R. A. (2012). Cross section restoration of salt-related deformation: Best practices and potential pitfalls. *Journal of Structural Geology*, *41*, 24–37. https://doi.org/10.1016/j.jsg.2011.12.012

Rowan, M. G., Tilton, J., Lebit, H., & Fiduk, J. C. (2022). Thin-skinned extensional salt tectonics, counter-regional faults, and the Albian Gap of Brazil. *Marine and Petroleum Geology*, *137*, 105478. https://doi.org/10.1016/j.marpetgeo.2021.105478

Samaila, N. K., & Likkason, O. K. (2013). Role of equatorial fracture zones on fluid migration across the South Atlantic Margins. *Journal of Earth Science and Climate Change*, *s12*(1), S12–S13. https://doi.org/10.4172/2157-7617.S12-004

Sanuade, O. A., Akanji, A. O., Olaojo, A. A., & Oyeyemi, K. D. (2018). Seismic interpretation and petrophysical evaluation of SH field, Niger Delta. *Journal of Petroleum Exploration and Production Technology*, *8*(1), 51–60. https://doi.org/10.1007/s13202-017-0363-x

Sapin, F., Ringenbach, J. C., & Clerc, C. (2021). Rifted margins classification and forcing parameters. *Scientific Reports*, *11*(1), 8199. https://doi.org/10.1038/s41598-021-87648-3

Sapin, F., Ringenbach, J.-C., Rives, T., & Pubellier, M. (2012). Counter-regional normal faults in a shale dominated deltas: Origin, mechanism and evolution. *Marine and Petroleum Geology*, *37*(1), 121–128. https://doi.org/10.1016/j.marpetgeo.2012.05.001

Schreckenberger, B., Hinz, K., Franke, D., Neben, S., & Roeser, H. A. (2002). Marine magnetic anomalies and the symmetry of the conjugated rifted margins of the South Atlantic. (Vols. *T52C–1217*, p. 83). American Geophysical Union, Fall Meeting, Supplement.

Schuster, D. C. (1995). Deformation of allochthonous salt and evolution of related salt-structural systems, eastern Louisiana Gulf Coast. In M. P. A. Jackson, D. G. Roberts, & S. Snelson (Eds.), *Salt Tectonics: A Global Perspective, American Association of Petroleum Geologists Memoir* (Vol. 65, pp. 177–198). American Association of Petroleum Geologists. https://doi.org/10.1306/M65604C8

Seton, M., Müller, R. D., Zahirovic, S., Williams, S., Wright, N., Cannon, J., et al. (2020). A global dataset of present-day oceanic crustal age and seafloor spreading parameters. *Geochemistry, Geophysics, Geosystems*, *21*(10), e2020GC009214. https://doi.org/10.1029/2020GC009214

Short, K. C., & Stäuble, A. J. (1967). Outline of geology of Niger Delta. *AAPG Bulletin*, *51*(5), 761–779. https://doi.org/10.1306/5D25C0CF-16C1-11D7-8645000102C1865D

Sibuet, J. C., & Mascle, J. (1978). Plate kinematic implications of Atlantic equatorial fracture zone trends. *Journal of Geophysical Research*, *83*(B7), 3401–3421. https://doi.org/10.1029/JB083iB07p03401

Sibuet, J.-C., Srivastava, S. P., & Spakman, W. (2004). Pyrenean orogeny and plate tectonics. *Journal of Geophysical Research: Solid Earth*, *109*(B8), B08104. https://doi.org/10.1029/2003JB002514

Soto, J. I., Déverchère, J., Hudec, M. R., Medaouri, M., Badji, R., Gaullier, V., & Leffondré, P. (2022). Crustal structures and salt tectonics on the margins of the western Algerian Basin (Mediterranean Region). *Marine and Petroleum Geology*, *144*, 105820. https://doi.org/10.1016/j.marpetgeo.2022.105820

Soto, J. I., Heidari, M., & Hudec, M. R. (2021). Proposal for a mechanical model of mobile shales. *Scientific Reports*, *11*(1), 23785. https://doi.org/10.1038/s41598-021-02868-x

Soto, J. I., & Hudec, M. R. (2023). Mud volcanoes guided by thrusting in compressional settings. *Geology*, *51*(8), 779–784. https://doi.org/10.1130/G51235.1

Soto, J. I., Hudec, M. R., Mondol, N. H., & Heidari, M. (2021). Shale transformations and physical properties–Implications for seismic expression of mobile shales. *Earth-Science Reviews*, *220*, 103746. https://doi.org/10.1016/j.earscirev.2021.103746

Spina, V. (2024). Seismic lines used in the study: Shale tectonics in the hyperextended continental margin of the Niger delta [Dataset]. *Figshare*. https://doi.org/10.6084/m9.figshare.27316476

Spina, V., & Mazzoli, S. (2023). Shale 3D flow and interaction with basement faults in the Niger Delta deep-water fold and thrust belt. *Tectonics*, *42*(12), e2023TC007957. https://doi.org/10.1029/2023TC007957

Stacher, P. (1995). Present understanding of the Niger Delta hydrocarbon habitat. In M. N. Oti & G. Postma (Eds.), *Geology of deltas* (pp. 257–267). A.A. Balkema.

Sun, Y., & Liu, L. (2018). Structural evolution of a thrust-related folds and associated fault systems in the eastern portion of the deep-water Niger Delta. *Marine and Petroleum Geology*, *92*, 285–307. https://doi.org/10.1016/j.marpetgeo.2017.12.012

Suppe, J. (2011). Mass balance and thrusting in detachment folds. In K. McClay, J. Shaw, & J. Suppe (Eds.), *Thrust fault-related folding, American Association of Petroleum Geologists Memoir* (Vol. 94, pp. 21–37). American Association of Petroleum Geologists. https://doi.org/10.1306/13251331M94389

Sutra, E., & Manatschal, G. (2012). How does the continental crust thin in a hyperextended rifted margin? *Geology*, *40*(2), 139–142. https://doi.org/10.1130/G32786.1

Swarbrick, R., O'Connor, S., & Lahann, R. (2011). Occurrence and prediction of high-pressure sediment along the West African margin. *The Leading Edge*, *30*(6), 682–687. https://doi.org/10.1190/1.3599155

Thiéblemont, D., Liégeois, J.-P., Fernández-Alonso, M., Ouabadi, A., Le Gall, B., Maury, R., et al. (2016). *Geological map of Africa (scale 1/10,000,000)*. Commission for the Geological Map of the World (CCGM), UNESCO, and the Geological Society of America.

Tingay, M., Bentham, P., De Feyter, A., & Kellner, A. (2012). Evidence for non–Andersonian faulting above evaporites in the Nile Delta. In D. Healy, R. W. H. Butler, Z. K. Shipton, & R. H. Sibson, (Eds.), *Faulting, Fracturing and Igneous Intrusion in the Earth's Crust* (Vol. 367(1), pp. 155–170). Geological Society, London, Special Publications. https://doi.org/10.1144/SP367.11

Tingay, M. R. P., Morley, C. K., Laird, A., Limpornipipat, O., Krisadasima, K., Pabchanda, S., & Macintyre, H. R. (2013). Evidence for overpressure generation by kerogene-to-gas maturation in the northern Malay Basin. *AAPG Bulletin*, *97*(4), 639–672. https://doi.org/10.1306/09041212032

Torsvik, T. H., Rousse, S., Labails, C., & Smethurst, M. A. (2009). A new scheme for the opening of the South Atlantic Ocean and the dissection of an Aptian salt basin. *Geophysical Journal International*, *177*(3), 1315–1333. https://doi.org/10.1111/j.1365-246X.2009.04137.x

Tuttle, M. L. W., Charpentier, R. R., & Brownfield, M. E. (1999). *The Niger Delta Petroleum System: Niger delta Province, Nigeria, Cameroon, and Equatorial Guinea, Africa* (Vol. 99–50–H, p. 65). U.S. Geological Survey, Denver, Open-File Report.

Van Rensbergen, P., & Morley, C. K. (2003). Re–evaluation of mobile shale occurrences on seismic sections of the Champion and Baram deltas, offshore Brunei. In P. Van Rensbergen, R. R. Hillis, A. J. Maltman, & C. K. Morley (Eds.), *Subsurface Sediment Mobilization, Geological Society of London, Special Publications* (Vol. 216(1), pp. 394–409). Geological Society of London. https://doi.org/10.1144/GSL.SP.2003.216.01.26

Van Rensbergen, P., Morley, C. K., Ang, D. W., Hoan, T. Q., & Lam, N. T. (1999). Structural evolution of shale diapirs from reactive rise to mud volcanism: 3D seismic data from the Baram delta, offshore Brunei Darussalam. *Journal of the Geological Society*, *156*(3), 633–650. https://doi.org/10.1144/gsjgs.156.3.0633

Vendeville, B. C. (2005). Salt tectonics driven by sediment progradation: Part 1–Mechanisms and kinematics. *AAPG Bulletin*, *89*(8), 1071–1079. https://doi.org/10.1306/03310503063

Whiteman, A. J. (1982). *Nigeria: Its petroleum geology, resources and potential, Volume 1*. Graham and Trotman.

Wiener, R. W., Mann, A., Angelich, M. T., & Molyneux, J. B. (2010). Mobile shale in the Niger delta: Characteristics, structure, and evolution. In L. Wood (Ed.), *Shale tectonics, American Association of Petroleum Geologists Memoir* (Vol. 93, pp. 145–161). American Association of Petroleum Geologists. https://doi.org/10.1306/13231313M933423

Winker, C. D., & Edwards, M. B. (1983). Unstable progradational clastic shelf margins. In D. J. Stanley & G. T. Moore (Eds.), *The Shelfbreak: Critical Interface on Continental Margins, The Society of Economic Paleontologists and Mineralogists (SEPM) Special Publication* (Vol. 33, pp. 139–157). Society of Economic Paleontologists and Mineralogists. https://doi.org/10.2110/pec.83.06.0139

Wu, J., McClay, K., & de Vera, J. (2020). Growth of triangle zone fold-thrusts within the NW Borneo deep-water fold belt, offshore Sabah, southern South China Sea. *Geosphere*, *16*(1), 329–356. https://doi.org/10.1130/GES02106.1

Wu, J. E., McClay, K., & Frankowicz, E. (2015). Niger Delta gravity-driven deformation above the relict Chain and Charcot Oceanic fracture zones, Gulf of Guinea: Insights from analogue. *Marine and Petroleum Geology*, *65*, 42–62. https://doi.org/10.1016/j.marpetgeo.2015.03.008

Wu, S., & Bally, A. W. (2000). Slope tectonics–Comparisons and contrasts of structural styles of salt and shale tectonics of the Northern Gulf of Mexico with shale tectonics of offshore Nigeria in Gulf of Guinea. In W. Mohriak & M. Talwani (Eds.), *Atlantic Rifts and Continental Margins* (Vol. 115, pp. 151–172). Geophysical Monograph, AGU. https://doi.org/10.1029/gm115p0151

Yassir, N., & Addis, M. A. (2002). Relationships between pore pressure and stress in different tectonic settings. In A. R. Huffman & G. L. Bowers (Eds.), *Pressure regimes in sedimentary basins and their prediction, American Association of Petroleum Geologists Memoir* (Vol. 76, pp. 79–88). American Association of Petroleum Geologists.

Yuan, X. P., Leroy, Y. M., & Maillot, B. (2020). Control of fluid pressures on the formation of listric normal faults. *Earth and Planetary Sciences Letters*, *529*, 115849. https://doi.org/10.1016/j.epsl.2019.115849

Zhang, J., Wu, S., Hu, G., Yue, D., Xu, Z., Chen, C., et al. (2021). Role of shale deformation in the structural development of a deepwater gravitational system in the Niger Delta. *Tectonics*, *40*(5), e2020TCT0046491. https://doi.org/10.1029/2020TC006491